[redacted]

[redacted]

Westinghouse Energy Systems

WESTINGHOUSE CLASS 3

WCAP-12396

ANALYSIS OF CAPSULE Y FROM THE COMMONWEALTH EDISON COMPANY ZION UNIT 2 REACTOR VESSEL RADIATION SURVEILLANCE PROGRAM

E. Terek
S. L. Anderson
L. Albertin

September 1989

Work performed under Shop Order No. CUAP-106

APPROVED: T. A. Meyer

T. A. Meyer, Manager
Structural Materials and Reliability Technology

Prepared by Westinghouse for the Commonwealth Edison Company

WESTINGHOUSE ELECTRIC CORPORATION
Nuclear and Advanced Technology Division
P.O. Box 2728
Pittsburgh, Pennsylvania 14230-2728

PREFACE

This report has been technically reviewed and verified.

	Reviewer	
Sections 1 through 5 and 7, 8	S. E. Yanichko	S. E. Yanichko
Section 6	E. P. Lippincott	E. P. Lippincott

TABLE OF CONTENTS

LIST OF ILLUSTRATIONS

LIST OF ILLUSTRATIONS (Cont)

LIST OF TABLES

LIST OF TABLES (Cont)

LIST OF TABLES (Cont)

SECTION 1
SUMMARY OF RESULTS

The analysis of the reactor vessel material contained in Capsule Y, the third surveillance capsule to be removed from the Commonwealth Edison Company Zion Unit 2 reactor pressure vessel, resulted in the following conclusions:

- The capsule received an average fast neutron fluence (E > 1.0 MeV) of 1.48×10^{19} n/cm^2.

- Irradiation of the reactor vessel lower shell Plate C4007-1, to 1.48×10^{19} n/cm^2 resulted in 30 and 50 ft-lb transition temperature increases of 121 and 130°F, respectively, for specimens oriented normal to the major working direction (transverse orientation) and temperature increases of 88 and 103°F, respectively, for specimens oriented parallel to the major working direction (longitudinal orientation).

- Weld metal irradiated to 1.48×10^{19} n/cm^2 experienced increases in the 30 and 50 ft-lb transition temperatures of 220 and 255°F, respectively. This results in a 30 ft-lb transition temperature of 210°F and a 50 ft-lb transition temperature of 300°F.

- Irradiation to 1.48×10^{19} n/cm^2 resulted in no decrease in the average upper shelf energy of Plate C4007-1 (transverse orientation) and a decrease of 18 ft-lb for the weld metal. This results in a weld metal average upper shelf energy of 51 ft-lb.

- Comparison of the 30 ft-lb transition temperature increases for the Zion Unit 2 surveillance material with predicted increases using the methods of NRC Regulatory Guide 1.99, Revision 2, demonstrated that the Plate C4007-1 material and weld metal transition temperature increases were 31° and 22°F, respectively, greater than predicted. NRC Regulatory Guide 1.99, Revision 2 requires a 2 sigma allowance, of 34°F for base metal and 56°F for weld metal, be added to the predicted

reference transition temperature to obtain a conservative upper bound value. Thus, the reference transition temperature increases for Plate C4007-1 material and the weld metal are bounded by the 2 sigma allowance for shift prediction.

SECTION 2
INTRODUCTION

This report presents the results of the examination of Capsule Y, the third capsule to be removed from the reactor in the continuing surveillance program which monitors the effects of neutron irradiation on the Commonwealth Edison Company Zion Unit 2 reactor pressure vessel materials under actual operating conditions.

The surveillance program for the Commonwealth Edison Company Zion Unit 2 reactor pressure vessel materials was designed and recommended by the Westinghouse Electric Corporation. A description of the surveillance program and the preirradiation mechanical properties of the reactor vessel materials are presented by Yanichko and Lege.[1] The surveillance program was planned to cover the 40-year design life of the reactor pressure vessel and was based on ASTM E-185-70, "Recommended Practice for Surveillance Tests in Nuclear Reactors". Westinghouse Electric Corporation personnel performed the postirradiation mechanical testing of the Charpy V-notch impact and tensile surveillance specimens.

This report summarizes testing and the postirradiation data obtained from surveillance Capsule Y removed from the Commonwealth Edison Company Zion Unit 2 reactor vessel and discusses the analysis of the data. The data are also compared to results of the previously removed Zion Unit 2 Capsule U[2] and Capsule T[3].

SECTION 3
BACKGROUND

The ability of the large steel pressure vessel, which contains the reactor core and its primary coolant to resist fracture constitutes an important factor in ensuring safety in the nuclear industry. The beltline region of the reactor pressure vessel is the most critical region of the vessel because it is subjected to significant fast neutron bombardment. The overall effects of fast neutron irradiation on the mechanical properties of low alloy ferritic pressure vessel steels such as SA533 Grade B Class 1 (base material of the Zion Unit 2 reactor pressure vessel beltline) are well documented in industry literature. Generally, low alloy ferritic materials demonstrate an increase in hardness and tensile properties and a decrease in ductility and toughness under certain conditions of irradiation.

A method for performing analyses to guard against fast fracture in reactor pressure vessels has been presented in "Protection Against Non-ductile Failure," Appendix G to Section III of the ASME Boiler and Pressure Vessel Code. The method utilizes fracture mechanics concepts and is based on the reference nil-ductility temperature (RT_{NDT}).

RT_{NDT} is defined as the greater of either the drop weight nil-ductility transition temperature (NDTT per ASTM E-208) or the temperature 60°F less than the 50 ft lb (and 35-mil lateral expansion) temperature as determined from Charpy specimens oriented normal (transverse) to the major working direction of the material. The RT_{NDT} of a given material is used to index that material to a reference stress intensity factor curve (K_{IR} curve) which appears in Appendix G of the ASME Code. The K_{IR} curve is a lower bound of dynamic, crack arrest, and static fracture toughness results obtained from several heats of pressure vessel steel. When a given material is indexed to the K_{IR} curve, allowable stress intensity factors can be obtained for this material as a function of temperature. Allowable operating limits can then be determined utilizing these allowable stress intensity factors.

RT_{NDT} and the operating limits of nuclear power plants can be adjusted to account for the effects of radiation on the reactor vessel material properties. The radiation embrittlement or changes in mechanical properties of a given reactor pressure vessel steel can be monitored by a reactor surveillance program such as the Commonwealth Edison Company Zion Unit 2 Reactor Vessel Radiation Surveillance Program.[1] A surveillance capsule is periodically removed from the operating nuclear reactor and the encapsulated specimens are tested. The increase in the average Charpy V-notch 30 ft lb temperature (ΔRT_{NDT}) due to irradiation is added to the original RT_{NDT} to adjust the RT_{NDT} for radiation embrittlement. This adjusted RT_{NDT} (RT_{NDT} initial + ΔRT_{NDT}) is used to index the material to the K_{IR} curve and to set operating limits for the nuclear power plant which reflect the effects of irradiation on the reactor vessel materials.

SECTION 4
DESCRIPTION OF PROGRAM

Eight surveillance capsules for monitoring the effects of neutron exposure on the Zion Unit 2 reactor pressure vessel core region material were inserted in the reactor vessel prior to initial plant startup. The capsules were positioned in the reactor vessel between the thermal shield and the vessel wall at locations shown in Figure 4-1. The vertical center of the capsules is opposite the vertical center of the core.

Capsule Y (Figure 4-2) was removed after 9.18 effective full power years of plant operation. This capsule contained Charpy V-notch impact and tensile specimens from the reactor vessel lower shell Plate C4007-1, and submerged arc weld metal representative of that used for the beltline region intermediate shell longitudinal weld seams of the reactor vessel and Charpy V-notch specimens from weld heat-affected zone (HAZ) material. All heat-affected zone specimens were obtained from within the HAZ of Plate C4007-1 of the representative weld. In addition, the capsule also contained Charpy V-notch specimens of an ASTM correlation monitor material (HSST Plate 02).

The chemical composition, toughness data and heat treatment of the surveillance material are presented in Tables 4-1 through Table 4-5. The chemical analyses reported in Table 4-1 were obtained from unirradiated material used in the surveillance program. In addition, a chemical analysis using Inductively Coupled Plasma Spectrometry (ICPS) was performed on irradiated Charpy specimens from the lower shell Plate C4007-1 and weld metal and is reported in Table 4-2. The chemistry results from the NBS certified reference standards are reported in table 4-3.

All test specimens were machined from the 1/4 thickness location of the plate. Test specimens represent material taken at least one plate thickness from the quenched end of the plate. All base metal Charpy V-notch impact and tensile specimens were oriented with the longitudinal axis of the specimen both normal to (transverse orientation) and parallel to (longitudinal orientation) the principal working direction of the plate. Charpy V-notch specimens from the

weld metal were oriented with the longitudinal axis of the specimens transverse to the weld direction. Tensile specimens were oriented with the longitudinal axis of the specimens normal to the welding direction. Weld metal IT Wedge Opening Loading test specimens in Capsule Y were machined such that the simulated crack in the specimen would propagate parallel to the weld direction for weld specimens. All specimens were fatigue precracked per ASTM E399-70T.

Capsule Y contained dosimeter wires of pure iron, copper, nickel, and unshielded aluminum-cobalt. In addition, cadmium-shielded dosimeters of Neptunium (Np^{237}) and Uranium (U^{238}) were contained in the capsule.

Thermal monitors made from two low-melting eutectic alloys and sealed in Pyrex tubes were included in the capsule and were located as shown in Figure 4-2. The two eutectic alloys and their melting points are:

2.5% Ag, 97.5% Pb	Melting Point 579°F (304°C)
1.75% Ag, 0.75% Sn, 97.5% Pb	Melting Point 590°F (310°C)

The arrangement of the various mechanical test specimens, dosimeters and thermal monitors contained in Capsule Y are shown in Figure 4-2.

TABLE 4-1

CHEMICAL COMPOSITION OF
THE ZION UNIT 2 REACTOR VESSEL
SURVEILLANCE MATERIALS

Element	Plate C4007-1[c] (Wt. %)	Weld Metal[b][c] (Wt. %)	ASTM Correlation Monitor Material
C	0.23	0.077	0.22
S	0.016	0.013	0.018
N_2	0.006	0.014	-
Co	0.001 (a)	0.001 (a)	-
Cu	0.12	0.28	0.14
Si	0.22	0.47	0.25
Mo	0.54	0.39	0.52
Ni	0.53	0.55	0.68
Mn	1.39	1.51	1.48
Cr	0.065	0.064	-
V	0.001	0.003	-
P	0.010	0.017	0.012
Sn	0.011	0.004	-
Al	0.033	0.030	-
Ti	0.001 (a)	0.001 (a)	-
Sb	0.001	0.001	-
Zr	0.001 (a)	0.001 (a)	-
As	0.008	0.003	-
B	0.003 (a)	0.003 (a)	-
Zn	0.001 (a)	0.003	-

(a) Not detected. The number indicates the minimum limit of detection.

(b) Surveillance weld specimens were made from same weld wire as the intermediate shell longitudinal weld seams (Wire Heat 72105) and Linde 80 Flux Lot 8773.

(c) Chemical composition data from WCAP-8132.

Table 4-2

CHEMICAL COMPOSITION FOR ZION UNIT 2 CAPSULE Y IRRADIATED CHARPY IMPACT SPECIMENS

Weld Metal Specimen No.	Chemical Composition (wt.%)[a] Cu	Ni	C	Mn	P	S	Si	Cr	Mo	V	Co
W-50	0.26	0.57	0.09	1.68	0.016	0.008	0.49	0.08	0.34	<0.010	0.016
W-55	0.27	0.60	0.09	1.57	0.021	0.007	0.45	0.07	0.41	<0.010	0.015
W-49	0.26	0.59	-	1.59	0.015	-	-	0.08	0.42	<0.010	0.015
W-51	0.28	0.60	-	1.58	0.020	-	-	0.08	0.40	<0.010	0.016
W-52	0.26	0.60	-	1.66	0.019	-	-	0.08	0.40	<0.010	0.015
w-53	0.27	0.60	-	1.67	0.018	-	-	0.08	0.39	<0.010	0.016
W-54	0.26	0.56	-	1.50	0.020	-	-	0.08	0.35	<0.010	0.015
W-56	0.23	0.59	-	1.60	0.020	-	-	0.08	0.40	<0.010	0.013

Plate C4007-1 Specimen No.	Cu	Ni	C	Mn	P	S	Si	Cr	Mo	V	Co
E-70	0.10	0.48	0.26	1.24	0.007	0.011	0.25	0.064	0.45	<0.010	0.010

(a) Method of analysis -- Inductively Coupled Plasma Spectrometry (ICPS) for all elements except C, S and Si.

TABLE 4-3
CHEMISTRY RESULTS FROM THE NBS
CERTIFIED REFERENCE STANDARDS

Material ID: Low Alloy Steel: NBS Certified Reference Standards

	NBS 361		NBS 362	
	Certified	Measured (a)	Certified	Measured (a)
Metals	Concentration in Weight Percent			
Fe *	95.6	(matrix)	95.3	(matrix)
Mn	0.66	0.678	1.04	1.053
Cr	0.694	0.732	0.30	0.307
Ni	2.00	above calib	0.59	0.602
Mo	0.19	0.211	0.068	0.056
Co	0.032	0.031	0.30	0.321
Cu	0.042	0.043	0.50	0.513
P	0.014	0.0147	0.041	0.0485
V	0.011	0.011	0.040	0.036
C	0.383	0.383	0.160	0.157
S	0.014	NA	0.036	0.0351

Material ID: Low Alloy Steel: NBS Certified Reference Standards

	NBS 363		NBS 364	
	Certified	Measured (a)	Certified	Measured (b)
Metals	Concentration in Weight Percent			
Fe *	94.4	(matrix)	96.7	(matrix)
Mn	1.50	1.543	0.255	0.261
Cr	1.31	1.396	0.063	0.064
Ni	0.30	0.319	0.144	0.147
Mo	0.028	0.032	0.49	0.520
Co	0.048	0.047	0.15	0.158
Cu	0.010	0.102	0.249	0.263
P	0.029	0.0283	0.01	0.0129
V	0.31	0.316	0.105	0.143
	0.62	NA	0.87	NA
S	0.0068	NA	0.0250	0.0249

* Matrix element calculated as difference for material balance.
Tentative value, certified ± 100% of value.
NA - Not analyzed; NR, Not requested

(a) Method of analysis -- Inductively Coupled Plasma Spectrometry (ICPS) for all elements except C, S and Si.

TABLE 4-4
ZION UNIT 2 REACTOR VESSEL TOUGHNESS DATA (UNIRRADIATED)

Component	Heat No.	Material Type	Cu (%)	Ni (%)	T_{NDT} (°F)	RT_{NDT} (°F)	NMWD(e) USE (FT-LB)
Closure Head Dome	B9094-1	A533B, Cl. 1	.14	.55	-20	11	72
Closure Head Seg.	C4787-1A	" "	.13	.62	0	0	88
Closure Head Seg.	C5086-2	" "	.09	.54	30	30	88
Closure Head Flange	124W609	A508, Cl. 2	.08	.70	12(a)	12	105
Vessel Flange	2V-965	" "	.12	.74	60(a)	60	79
Inlet Nozzle	ZT4007-2	" "	.11	.70	48(a)	48	>78
Inlet Nozzle	ZT3885-1	" "	.11	.58	60(a)	60	82
Inlet Nozzle	ZT3885	" "	.11	.56	43(a)	43	78
Inlet Nozzle	ZT3885	" "	.11	.56	60(a)	60	>84
Outlet Nozzle	ZV3930	" "	.12	.66	58(a)	58	93
Outlet Nozzle	ZV3930	" "	.11	.65	48(a)	48	>80
Outlet Nozzle	ZV3930	" "	.12	.67	55(a)	55	84
Outlet Nozzle	ZT3885-4	" "	.11	.57	60(a)	60	>61
Upper Nozzle Shell	ZD3940	A508, Cl. 2	.07	.62	10	10	106
Lower Nozzle Shell	ZV3855	" "	.09	.66	10	10	>80
Lower Shell	B8029-1	A533B, Cl. 1	.12	.51	-10	22	81
Lower Shell	C4007-1	" "	.12	.53	10	22	94 (Actual)
Inter. Shell	B8006-1	" "	.12	.54	10	10	89
Inter. Shell	B8040-1	" "	.14	.52	-10	2	92
Bottom Head Trans. Ring	3V-433	A508, Cl. 2	.09	.76	0	0	87
Bottom Head Dome	C4007-2	A533B, Cl. 1	.12	.53	-20	0	72
Inter. to Lower Shell Girth Weld Seam	SA1769 (b)	SAW	.26	.60	0(a)	0	-
Lower Shell Long. Weld Seams	WF29 (c)	SAW	.23	.63	0(a)	0	-
Inter. Shell Long. Weld Seams	WF70 (d)	SAW	.32	.56	0(a)	0	-

(a) Estimated using method of U.S. NRC NUREG-0800 Branch Technical Position MTEB 5-2, July, 1981.
(b) Weld Wire Heat No. 71249 and Linde 80 Flux Lot No. 8738
(c) Weld Wire Heat No. 72102 and Linde 80 Flux Lot No. 8650
(d) Weld Wire Heat No. 72105 and Linde 80 Flux Lot No. 8669 (Chemical composition per WCAP-10962, December 1985)
(e) Normal to Major Working direction

TABLE 4-5

HEAT TREATMENT OF THE ZION UNIT 2
REACTOR VESSEL SURVEILLANCE MATERIALS

Material	Temperature (°F)	Time (hr)	Coolant
Intermediate Shell	1600/1650	9 3/4	Brine quenched
Plate C4007-1	1200/1225	9 3/4	Brine quenched
	1100/1150	30	Furnace cooled
Weld Metal	1100/1150	30	Furnace cooled
Correlation Monitor	1625 ± 25	4	Air cooled
(HSST Plate 02)	1600 ± 25	4	Water quenched
	1225 ± 25	4	Furnace cooled
	1150 ± 25	10	Furnace cooled

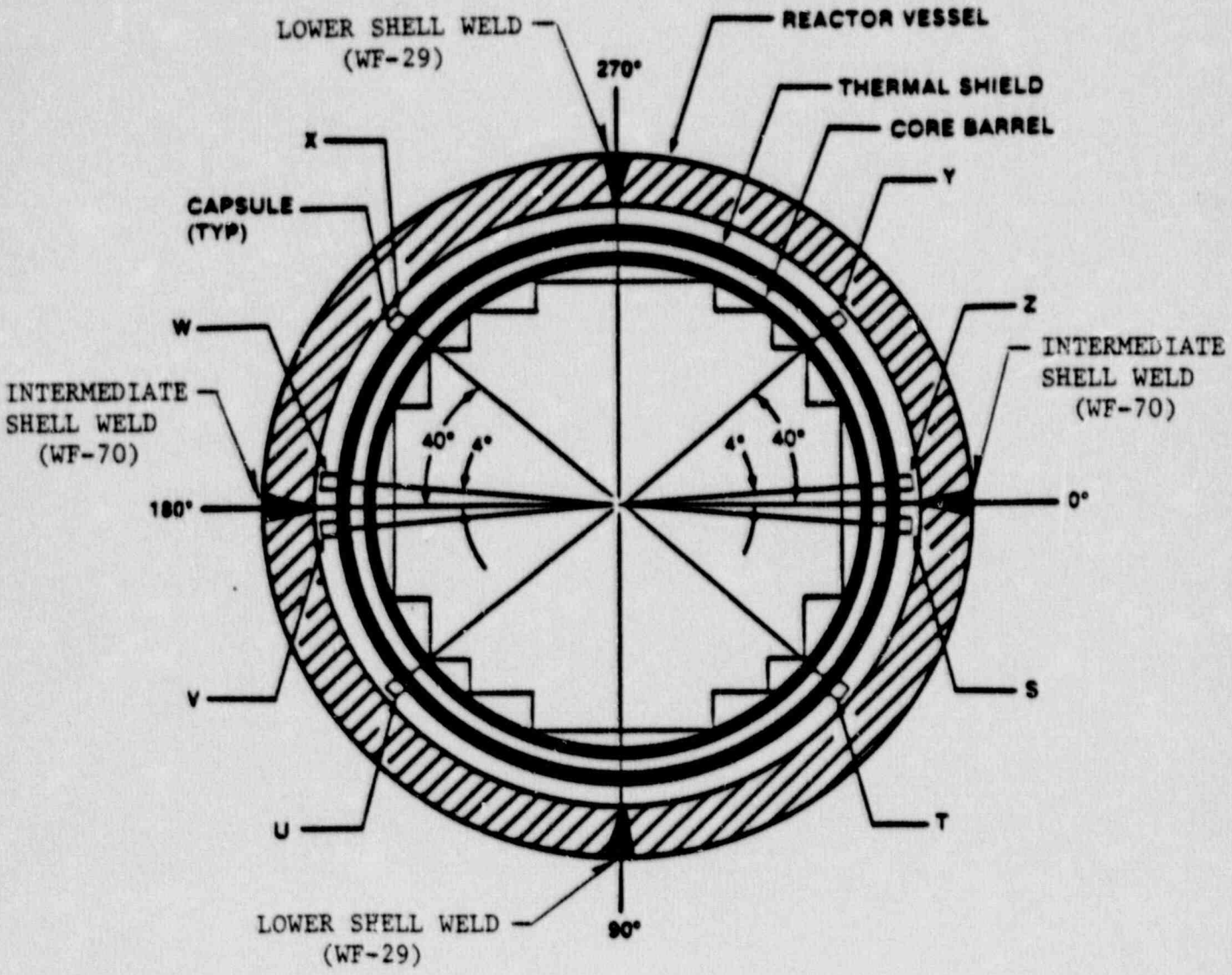

Figure 4-1. Arrangement of Surveillance Capsules in the Zion Unit 2 Reactor Vessel

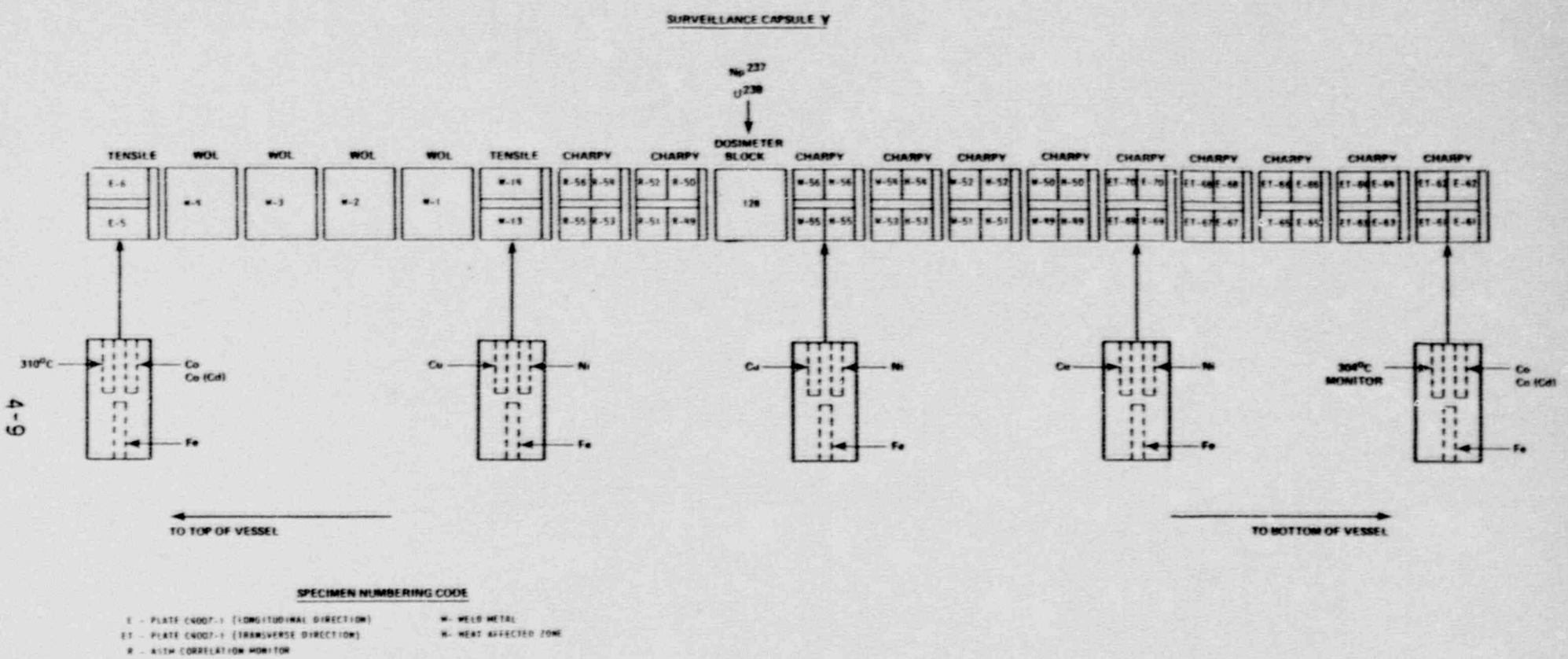

Figure 4-2 Capsule Y Diagram Showing Locations of Specimens, Thermal Monitors, and Dosimeters

SECTION 5
TESTING OF SPECIMENS FROM CAPSULE Y

5-1. OVERVIEW

The postirradiation mechanical testing of the Charpy V-notch and tensile specimens was performed at the Westinghouse Research and Development Laboratory with consultation by Westinghouse Nuclear Energy Systems personnel. Testing was performed in accordance with 10CFR50, Appendices G and H[4], ASTM Specification E185-82 and Westinghouse Procedure MHL 8402, Revision 1 as modified by Westinghouse RMF Procedures 8102, Revision 1 and 8103, Revision 1.

Upon receipt of the capsule at the laboratory, the specimens and spacer blocks were carefully removed, inspected for identification number, and checked against the master list in WCAP-8132.[1] No discrepancies were found.

Examination of the two low-melting 304°C (579°F) and 310°C (590°F) eutectic alloys indicated no melting of either type of thermal monitor. Based on this examination, the maximum temperature to which the test specimens were exposed was less than 304°C (579°F).

The Charpy impact tests were performed per ASTM Specification E23-82 and RMF Procedure 8103, Revision 1 on a Tinius-Olsen Model 74, 358J machine. The tup (striker) of the Charpy machine is instrumented with an Effects Technology model 500 instrumentation system. With this system, load-time and energy-time signals can be recorded in addition to the standard measurement of Charpy energy (E_D). From the load-time curve, the load of general yielding (P_{GY}), the time to general yielding (t_{GY}), the maximum load (P_M), and the time to maximum load (t_M) can be determined. Under some test conditions, a sharp drop in load indicative of fast fracture was observed. The load at which fast fracture was initiated is identified as the fast fracture load (P_F), and the load at which fast fracture terminated is identified as the arrest load (P_A). The Charpy machine is maintained and

calibrated in accordance with ASTM Specification E-23. The annual qualification of the Charpy machine is accomplished with the Standardized Watertown test specimens. The specimens and procedures used by Westinghouse are recommended by the Army Materials Technology Laboratory and is identical to the approached used to certify machines that generate data for government contracts.

The energy at maximum load (E_M) was determined by comparing the energy-time record and the load-time record. The energy at maximum load is approximately equivalent to the energy required to initiate a crack in the specimen. Therefore, the propagation energy for the crack (E_p) is the difference between the total energy to fracture (E_D) and the energy at maximum load.

The yield stress (σy) is calculated from the three point bend formula. The flow stress is calculated from the average of the yield and maximum loads, also using the three point bend formula.

Percentage shear was determined from postfracture photographs using the ratio-of-areas methods in compliance with ASTM Specification A370-77. The lateral expansion was measured using a dial gage rig similar to that shown in the same specification.

Tension tests were performed on a 20,000-pound Instron, split-console test machine (Model 1115) per ASTM Specifications E8-83 and E21-79, and RMF Procedure 8102, Revision 1. All pull rods, grips, and pins were made of Inconel 718 hardened to Rc45. The upper pull rod was connected through a universal joint to improve axiality of loading. The tests were conducted at a constant crosshead speed of 0.05 inch per minute throughout the test.

Deflection measurements were made with a linear variable displacement transducer (LVDT) extensometer. The extensometer knife edges were spring-loaded to the specimen and operated through specimen failure. The extensometer gage length is 1.00 inch. The extensometer is rated as Class B-2 per ASTM E83-67.

Elevated test temperatures were obtained with a three-zone electric resistance split-tube furnace with a 9-inch hot zone. All tests were conducted in air.

Because of the difficulty in remotely attaching a thermocouple directly to the specimen, the following procedure was used to monitor specimen temperature. Chromel-alumel thermocouples were inserted in shallow holes in the center and each end of the gage section of a dummy specimen and in each grip. In test configuration, with a slight load on the specimen, a plot of specimen temperature versus upper and lower grip and controller temperatures was developed over the range room temperature to 550°F (288°C). The upper grip was used to control the furnace temperature. During the actual testing the grip temperatures were used to obtain desired specimen temperatures. Experiments indicated that this method is accurate to plus or minus 2°F.

The yield load, ultimate load, fracture load, total elongation, and uniform elongation were determined directly from the load-extension curve. The yield strength, ultimate strength, and fracture strength were calculated using the original cross-sectional area. The final diameter and final gage length were determined from postfracture photographs. The fracture area used to calculate the fracture stress (true stress at fracture) and percent reduction in area was computed using the final diameter measurement.

5.2. CHARPY V-NOTCH IMPACT TEST RESULTS

The results of Charpy V-notch impact tests performed on the various materials contained in Capsule Y irradiated to approximately 1.48×10^{19} n/cm^2 at 550°F are presented in Tables 5-1 through 5-6 and Figures 5-1 through 5-5. The transition temperature increases and upper shelf energy decreases for the Capsule Y material are shown in Table 5-7.

Irradiation of the vessel lower shell Plate C4007-1 material (transverse orientation) specimens to 1.48×10^{19} n/cm^2 (Figure 5-1) resulted in a 30 and 50 ft-lb transition temperature increases of 121°F and 130°F, respectively, and an upper shelf energy increase of 4 ft-lb when compared to the unirradiated data.[1] It is probable that the increase in upper shelf energy is due to a random scatter in the data and it is more likely that the upper shelf energy is not changed.

Irradiation of the vessel lower shell Plate C4007-1 material (longitudinal orientation) specimens to 1.48×10^{19} m/cm^2 (Figure 5-2) resulted in 30 and 50 ft-lb transition temperature increases of 88°F and 103°F, respectively, and an upper shelf energy decrease of 17 ft-lb when compared to the unirradiated data.

Weld material irradiated to 1.48×10^{19} n/cm^2 (Figure 5-3) resulted in a 30 ft-lb transition temperature increase of 220°F (from -10°F to 210°F) and a 50 ft-lb transition temperature increase of 255°F (from 45°F to 300°F). Weld metal irradiated to 1.48×10^{19} n/cm^2 resulted in an upper shelf energy decrease of 18 ft-lb (from 69 ft-lb to 51 ft-lb).

Weld HAZ metal irradiated to 1.48×10^{19} n/cm^2 (Figure 5-4) resulted in 30 and 50 ft-lb transition temperature increases of 97°F and 99°F, respectively, and an upper shelf energy decrease of 24 ft-lb.

A533 Grade B Class 1 correlation monitor material (HSST Plate 02) irradiated to 1.48×10^{19} n/cm^2 (Figure 5-5) resulted in 30 and 50 ft-lb transition temperature increases of 135°F and 137°F, respectively, and an upper shelf energy decrease of 14 ft-lb. The 30 ft-lb transition temperature increase is 23°F greater than predicted. The 23°F increase is bounded by the 2 sigma allowance of 34°F for shift prediction.

The fracture appearance of each irradiated Charpy specimen from the various materials is shown in Figures 5-6 through 5-10 and show an increasing ductile or tougher appearance with increasing test temperature.

Table 5-8 shows a comparison of the 30 ft-lb transition temperature (ΔRT_{NDT}) increases for the various Zion Unit 2 surveillance materials with predicted increases using the methods of NRC Regulatory Guide 1.99, Revision 2.[5] This comparison shows that the transition temperature increase resulting from irradiation to 1.48×10^{19} n/cm^2 is greater than predicted by the Guide for Plate C4007-1. The weld metal transition temperature increase resulting from 1.48×10^{19} n/cm^2 is also greater than the Regulatory Guide prediction.

5-3. TENSION TEST RESULTS

The results of tension tests performed on Plate C4007-1 (longitudinal orientation) and weld metal irradiated to 1.48×10^{19} n/cm^2 are shown in Table 5-5 and Figures 5-11 and 5-12, respectively. These results show that irradiation produced a 0.2 percent yield strength increase of approximately 20 ksi for Plate C4007-1 and the weld metal. Fractured tension specimens for each of the materials are shown in Figures 5-13 and 5-14. A typical stress-strain curve for the tension specimens is shown in Figure 5-15.

5-4. WEDGE OPENING LOADING

It is common practice to store 1T - Wedge Opening Loading (WOL) fracture mechanics specimens at the Westinghouse Science and Technology Center Hot Cell.

TABLE 5-1

CHARPY V-NOTCH IMPACT DATA FOR THE ZION UNIT 2
REACTOR VESSEL SHELL PLATE C4007-1
IRRADIATED AT 550°F, FLUENCE 1.48 x 10^{19} n/cm^2 (E > 1.0 MeV)

Sample No.	Temperature (°F)	(°C)	Impact Energy (ft-lb)	(J)	Lateral Expansion (mils)	(mm)	Shear (%)
			Longitudinal Orientation				
E62	75	(24)	12.0	(16.5)	10.0	(0.25)	10
E61	125	(52)	32.0	(43.5)	27.0	(0.69)	20
E70	125	(52)	31.0	(42.0)	22.0	(0.56)	20
E63	150	(66)	47.0	(63.5)	35.0	(0.89)	35
E66	150	(66)	44.0	(59.5)	34.0	(0.86)	35
E67	175	(79)	53.0	(72.0)	41.0	(1.05)	45
E65	200	(93)	69.0	(93.5)	45.0	(1.14)	70
E69	275	(135)	113.0	(153.0)	60.0	(1.52)	100
E64	350	(177)	108.0	(146.5)	73.0	(1.85)	100
E68	450	(232)	112.0	(152.0)	73.0	(1.85)	100
			Transverse Orientation				
ET62	75	(24)	14.0	(19.0)	14.0	(0.36)	10
ET61	150	(66)	23.0	(31.0)	22.0	(0.56)	20
ET67	175	(79)	35.0	(47.5)	30.0	(0.76)	30
ET66	175	(79)	35.0	(47.5)	32.0	(0.81)	25
ET70	200	(93)	43.0	(58.5)	35.0	(0.89)	45
ET65	210	(99)	94.0	(127.5)	68.0	(1.73)	100
ET68	240	(116)	83.0	(112.5)	60.0	(1.52)	80
ET64	275	(135)	78.0	(106.0)	59.0	(1.50)	80
ET69	350	(177)	102.0	(138.5)	67.0	(1.70)	100
ET6_	450	(232)	98.0	(133.0)	66.0	(1.68)	100

TABLE 5-2

CHARPY V-NOTCH IMPACT DATA FOR THE ZION UNIT 2
REACTOR VESSEL WELD METAL AND HAZ METAL IRRADIATED AT 550°F
FLUENCE 1.48 x 10^{19} n/cm^2 (E > 1.0 MeV)

Sample No.	Temperature (°F)	(°C)	Impact Energy (ft-lb)	(J)	Lateral Expansion (mils)	(mm)	Shear
			Weld Metal				
W56	74	(23)	15.0	(20.5)	10.0		
W55	150	(66)	19.0	(26.0)	15.0		
W50	200	(93)	20.0	(27.0)	9		
W53	225	(107)	39.0	(53.0)	[illegible]		
W54	225	(107)	33.0	(44.5)	[illegible].0		
W52	250	(121)	44.0	(59.5	[illegible].0	([illegible]	
W49	350	(177)	50.0	(68.0	0	(1.07)	
W51	450	(232)	52.0	(70-5	.0	(1.[illegible]	[illegible]
			HAZ Metal				
H54	-50	(-46)	23.0	(31.0)	19.0	(0.48)	10
H55	-10	(-23)	10.0	(13.5)	14.0	(0.36)	10
H56	0	(-18)	38.0	(51.5)	27.0	(0.69)	30
H49	25	(- 4)	49.0	(66.5)	33.0	(0.84)	45
H51	75	(24)	48.0	(65.0)	29 0	(0.74)	40
H52	150	(66)	95.0	(129.0)	70.0	(1.78)	100
H50	250	(121)	118.0	(160.0)	76.0	(1.93)	100
H53	350	(177)	83.0	(112.5)	53.0	(1.35)	100

TABLE 5-3

CHARPY V-NOTCH IMPACT DATA FOR THE ZION UNIT 2
ASTM CORRELATION MONITOR MATERIAL (HSST PLATE 02)
IRRADIATED AT 550°F, FLUENCE 1.48 x 10^{19} n/cm^2 (E > 1.0 MeV)

Sample No.	Temperature (°F)	(°C)	Impact Energy (ft-lb)	(J)	Lateral Expansion (mils)	(mm)	Shear (%)
R55	74	(23)	14.0	(19.0)	11.0	(0.28)	10
R51	150	(66)	18.0	(24.5)	15.0	(0.38)	15
R54	175	(79)	23.0	(31.0)	21.0	(0.53)	20
R49	200	(93)	43.0	(58.5)	31.0	(0.79)	35
R50	200	(93)	39.0	(53.0)	29.0	(0.74)	35
R56	250	(121)	75.0	(101.5)	53.0	(1.35)	65
R56	350	(177)	113.0	(153.0)	74.0	(1.88)	100
R52	450	(232)	108.0	(146.0)	70.0	(1.78)	100

TABLE 5-4

INSTRUMENTED CHARPY IMPACT TEST RESULTS FOR ZION UNIT 2

REACTOR VESSEL SHELL PLATE C4007-1

IRRADIATED AT 550°F, FLUENCE 1.48 x 10^{19} n/cm^2 (E > 1.0 MeV)

Sample Number	Test Temp (°F)	Charpy Energy (ft-lb)	Normalized Energies (ft-lb/in^2) Charpy Ed/A	Maximum Em/A	Prop Ep/A	Yield Load (kips)	Time to Yield (μsec)	Maximum Load (kips)	Time to Maximum (μsec)	Fracture Load (kips)	Arrest Load (kips)	Yield Stress (ksi)	Flow Stress (ksi)
Longitudinal Orientation													
E62	75	12.0	97	39	58	2.75	80	3.60	135	3.45	0.45	92	105
E70	125	31.0	250	151	99	2.95	85	4.25	360	4.25	0.65	98	119
E61	125	32.0	258	169	88	2.25	95	3.90	445	3.90	1.05	74	102
E66	150	44.0	354	217	138	2.70	85	4.20	510	4.10	1.15	90	115
E63	150	47.0	378	206	173	2.60	90	4.00	510	3.95	1.45	86	109
E67	175	53.0	427	253	174	3.00	60	3.85	610	3.85	1.45	100	114
E65	200	69.0	556	266	290	2.55	60	4.40	575	4.15	2.05	84	115
E69	275	113.0	910	298	612	2.55	145	4.15	750	-	-	84	111
E64	350	108.0	870	266	604	3.00	100	4.20	610	-	-	99	119
E68	450	112.0	902	259	642	2.60	110	4.05	625	-	-	97	115
Transverse Orientation													
ET62	75	14.0	113	55	58	3.45	45	3.95	130	3.95	0.15	114	122
ET61	150	23.0	185	94	91	2.45	65	3.65	260	3.65	1.05	80	100
ET66	175	35.0	282	142	139	2.30	80	3.80	375	3.75	1.55	76	101
ET67	175	35.0	282	159	123	2.80	65	4.15	370	4.10	1.25	93	115
ET70	200	43.0	346	176	171	3.30	95	4.20	410	4.15	1.95	109	124
ET65	210	94.0	757	220	537	2.70	130	3.65	605	-	-	89	105
ET68	240	83.0	668	239	429	2.45	110	4.15	575	3.80	2.90	81	109
ET64	275	78.0	628	173	455	2.20	80	3.65	480	-	-	72	96
ET69	350	102.0	821	258	563	2.90	105	4.15	605	-	-	96	117
ET63	450	98.0	789	209	580	2.85	95	4.00	505	-	-	95	113

TABLE 5-5

INSTRUMENTED CHARPY IMPACT TEST RESULTS FOR ZION UNIT 2

REACTOR VESSEL WELD METAL AND HAZ METAL

IRRADIATED AT 550°F, FLUENCE 1.48 x 10^{19} n/cm^2 (E > 1.0 MeV)

Sample Number	Test Temp (°F)	Charpy Energy (ft-lb)	Normalized Energies (ft-lb/in^2) Charpy Ed/A	Maximum Em/A	Prop Ep/A	Yield Load (kips)	Time to Yield (μsec)	Maximum Load (kips)	Time to Maximum (μsec)	Fracture Load (kips)	Arrest Load (kips)	Yield Stress (ksi)	Flow Stress (ksi)
							Weld Metal						
W56	74	15.0	121	72	49	2.95	85	4.35	185	4.35	0.15	98	121
W55	150	19.0	153	99	54	3.40	95	3.80	255	3.80	0.90	113	119
W50	200	20.0	161	95	66	3.70	95	4.10	230	4.10	1.70	123	129
W54	225	33.0	266	126	140	2.75	90	3.75	335	3.75	2.85	90	107
W53	225	39.0	314	130	184	2.65	115	3.65	370	3.65	3.30	87	104
W52	250	44.0	354	152	202	3.60	90	4.35	355	-	-	119	131
W49	350	50.0	403	170	233	3.50	60	4.25	360	-	-	116	128
W51	450	52.0	419	159	260	3.30	95	3.85	380	-	-	109	118
							HAZ Metal						
H54	-50	23.0	185	111	75	3.00	100	4.15	285	4.15	0.30	98	118
H55	-10	10.0	81	45	36	2.35	40	3.05	125	3.05	-	78	89
H56	0	38.0	306	177	129	2.09	80	4.10	410	4.10	1.15	95	116
H49	25	49.0	395	216	178	2.55	75	4.80	470	4.55	1.50	84	122
H51	75	48.0	387	235	152	2.75	70	4.50	500	4.35	1.00	91	120
H52	150	95.0	765	220	545	3.30	90	4.15	505	-	-	109	123
H50	250	118.0	950	303	647	3.30	90	4.30	655	-	-	109	126
H53	350	93.0	668	221	448	2.75	85	4.15	520	-	-	91	114

TABLE 5-6

INSTRUMENTED CHARPY IMPACT TEST RESULTS FOR ZION UNIT 2

ASTM CORRELATION MONITOR MATERIAL (HSST PLATE 02)

IRRADIATED AT 550°F, FLUENCE 1.48 x 10^{19} n/cm^2 (E > 1.0 MeV)

Sample Number	Test Temp (°F)	Charpy Energy (ft-lb)	Normalized Energies (ft-lb/in^2) Charpy Ed/A	Maximum Em/A	Prop Ep/A	Yield Load (kips)	Time to Yield (μsec)	Maximum Load (kips)	Time to Maximum (μsec)	Fracture Load (kips)	Arrest Load (kips)	Yield Stress (ksi)	Flow Stress (ksi)
R55	74	14.0	113	46	67	2.55	100	3.90	155	3.95	0.30	84	106
R51	150	18.0	145	83	62	2.40	60	3.45	235	3.45	0.55	79	97
R54	175	23.0	185	90	95	2.10	90	3.40	285	3.40	1.25	69	91
R50	200	39.0	314	216	98	2.75	85	4.25	505	4.25	1.60	91	116
R49	200	43.0	346	246	100	2.30	60	4.05	580	4.05	1.20	77	105
R56	250	75.0	604	220	384	3.15	100	4.15	510	-	-	105	121
R53	350	113.0	910	284	626	2.50	65	4.05	665	-	-	82	108
R52	450	108.0	870	242	628	2.75	95	3.80	605	-	-	90	108

TABLE 5-7
THE EFFECT OF 550°F IRRADIATION AT 1.48 x 10^{19} n/cm^2 (E > 1.0 MeV) ON THE NOTCH TOUGHNESS PROPERTIES OF THE ZION UNIT 2 REACTOR VESSEL MATERIALS

Material	Average 30 ft-lb Temp (°F)			Average 35 mil Lateral Expansion Temp (°F)			Average 50 ft-lb Temp (°F)			Average Energy Absorption at Full Shear (ft-lb)		
	Unirradiated	Irradiated	ΔT	Unirradiated	Irradiated	ΔT	Unirradiated	Irradiated	ΔT	Unirradiated	Irradiated	Δ(ft-lb)
Plate C4007-1 (Longitudinal)	37	125	88	50	160	110	62	165	103	128	111	-17
Plate C4007-1 (Transverse)	49	170	121	65	190	125	80	210	130	94	98	+4
Weld Metal	-10	210	220	0	240	240	45	300	255	69	51	-18
HAZ Metal	-87	10	97	-45	50	95	-39	60	99	123	99	-24
Correlation Monitor	50	185	135	62	212	150	78	215	137	124	110	-14

TABLE 5-8

COMPARISON OF ZION UNIT 2
REACTOR VESSEL SURVEILLANCE CAPSULE CHARPY IMPACT TEST RESULTS
WITH REGULATORY GUIDE 1.99 REVISION 2 PREDICTIONS

Material	Capsule	Fluence[a] 10^{19} n/cm^2	ΔRT_{NDT} (°F)		USE DECREASE (%)	
			Meas.	Pred.	Meas.	Pred.
Plate C4007-1	U	0.27	38	53.3	5.5	16
(Longitudinal)	T	0.78	75	76.3	18.8	19
	Y	1.48	88	91.0	13.3	22.5
Plate C4007-1	U	0.27	49	53.3	0	16
(Transverse)	T	0.78	90	76.3	14.9	19
	Y	1.48	121	91.0	0	22.5
Weld Metal	U	0.27	128	117	27.5	32
	T	0.78	175	167	36.2	40
	Y	1.48	220	200	26.1	46
Correlation	U	0.27	50	66.3	10.5	17.5
Monitor	T	0.78	100	94.9	28.2	22
	Y	1.48	135	113	11.3	25.5

[a] These have been recalculated using the methods of Section 6.

TABLE 5-9

TENSILE PROPERTIES FOR ZION UNIT 2

REACTOR VESSEL MATERIAL IRRADIATED TO 1.48 x 10^{19} n/cm^2 (E > 1.0 MeV)

Material	Sample Number	Test Temp. (°F)	0.2% Yield Strength (ksi)	Ultimate Strength (ksi)	Fracture Load (kip)	Fracture Stress (ksi)	Fracture Strength (ksi)	Uniform Elongation (%)	Total Elongation (%)	Reduction in Area (%)
Plate C4007-1 (Long. Orient.)	E6	79	89.1	114.1	3.60	220.6	73.3	11.2	23.2	68
	E5	550	75.4	99.8	3.40	189.1	69.3	9.6	20.3	63
Weld	W14	79	91.7	114.1	4.27	254.1	86.9	9.1	19.5	66
	W13	550	89.6	105.9	4.60	210.8	93.7	8.3	13.5	56

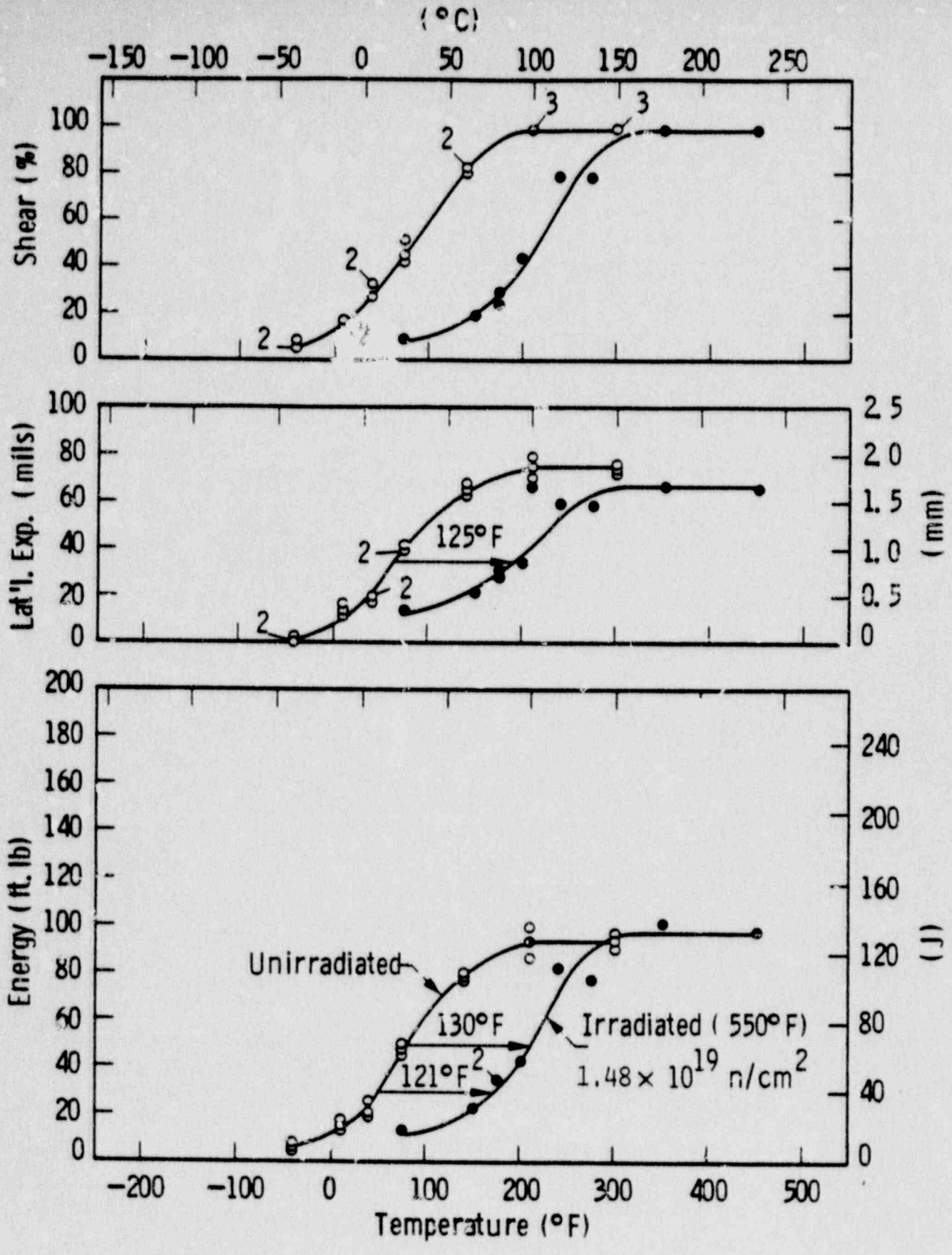

FIGURE 5-1 CHARPY V-NOTCH IMPACT DATA FOR ZION UNIT 2 REACTOR VESSEL SHELL PLATE C4007-1 (TRANSVERSE ORIENTATION)

Curve 757563-A

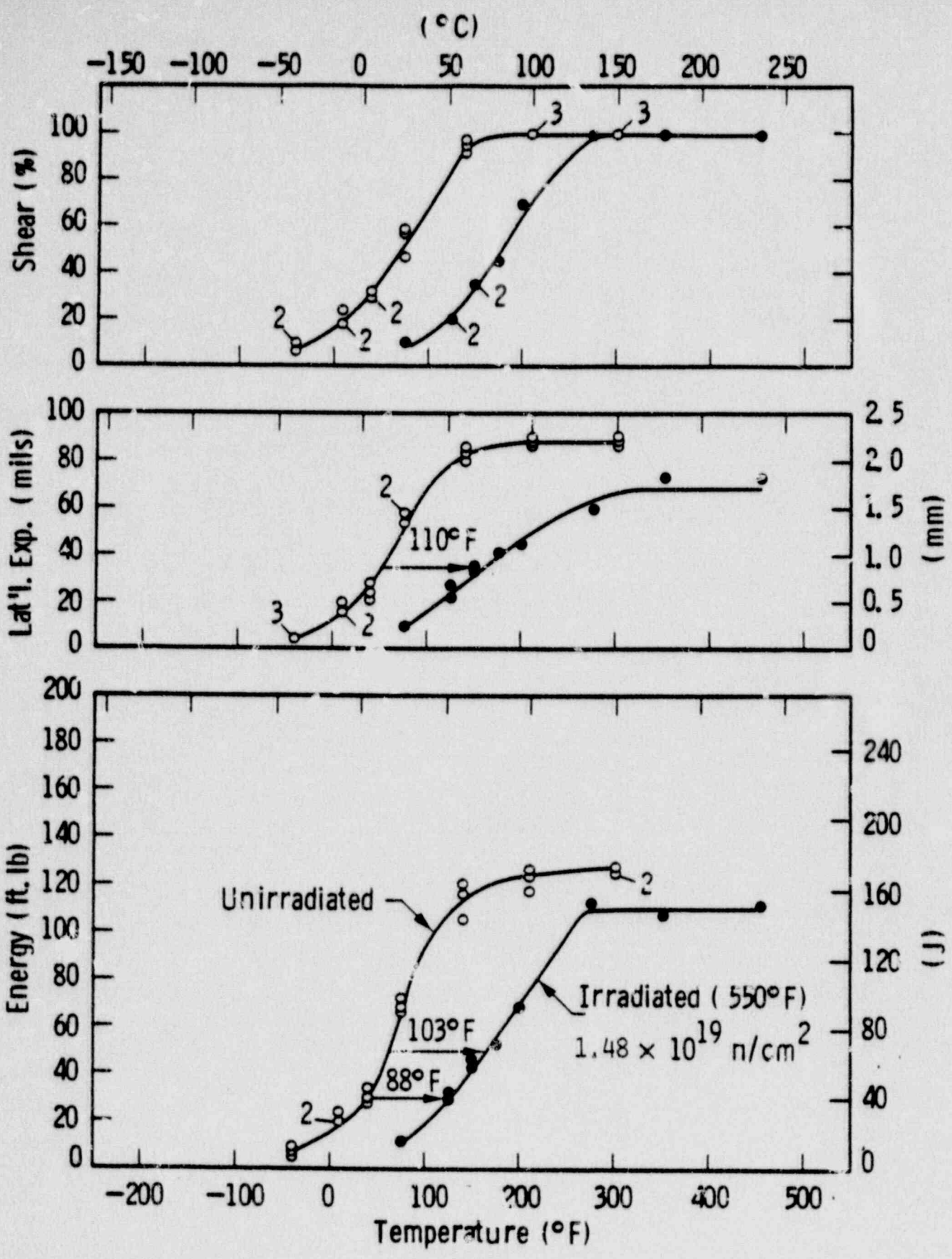

FIGURE 5-2 CHARPY V-NOTCH IMPACT DATA FOR ZION UNIT 2 REACTOR VESSEL SHELL PLATE C4007-1 (LONGITUDINAL ORIENTATION)

Curve 757564-A

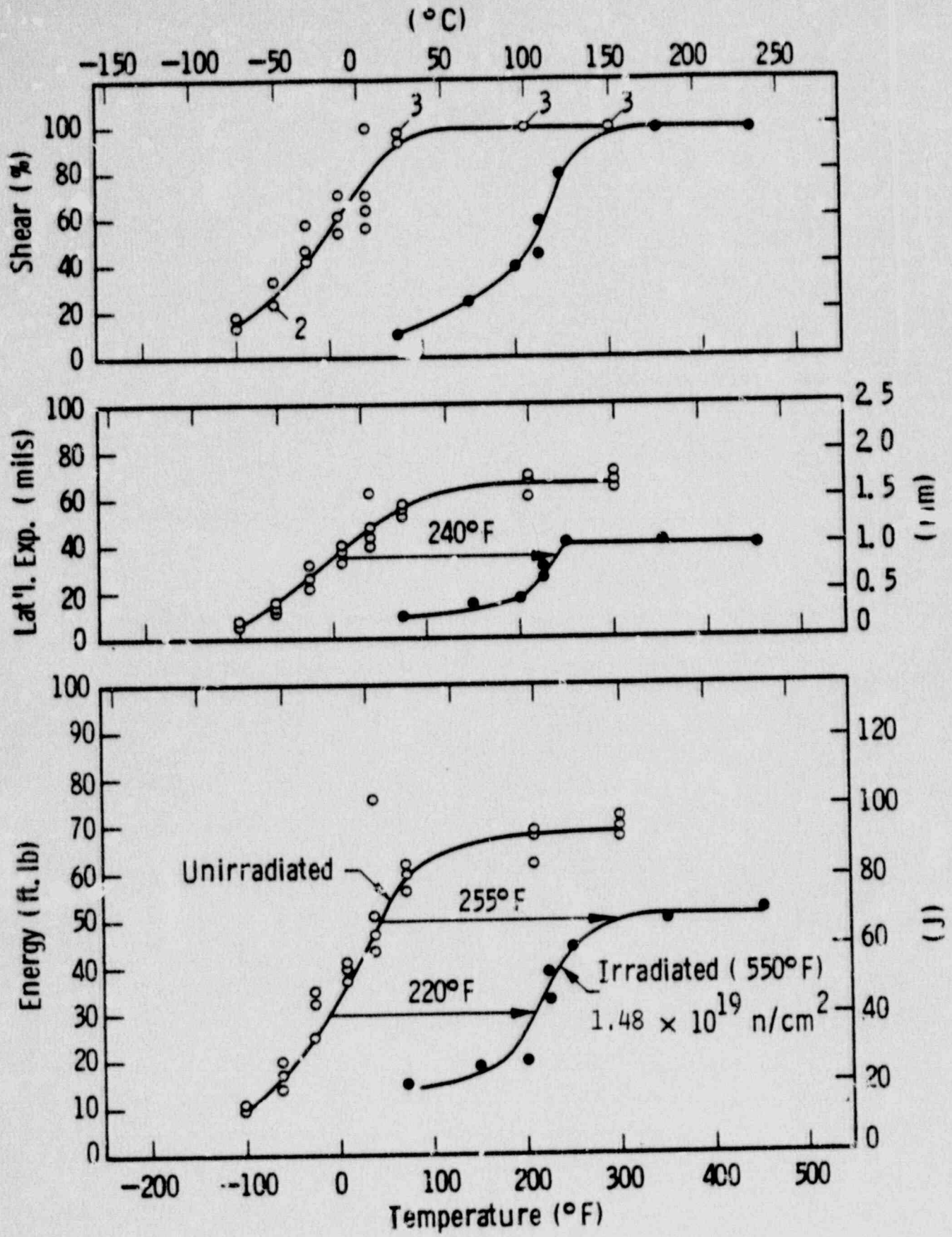

FIGURE 5-3 CHARPY V-NOTCH IMPACT DATA FOR ZION UNIT 2 REACTOR VESSEL WELD METAL

Curve 757562-A

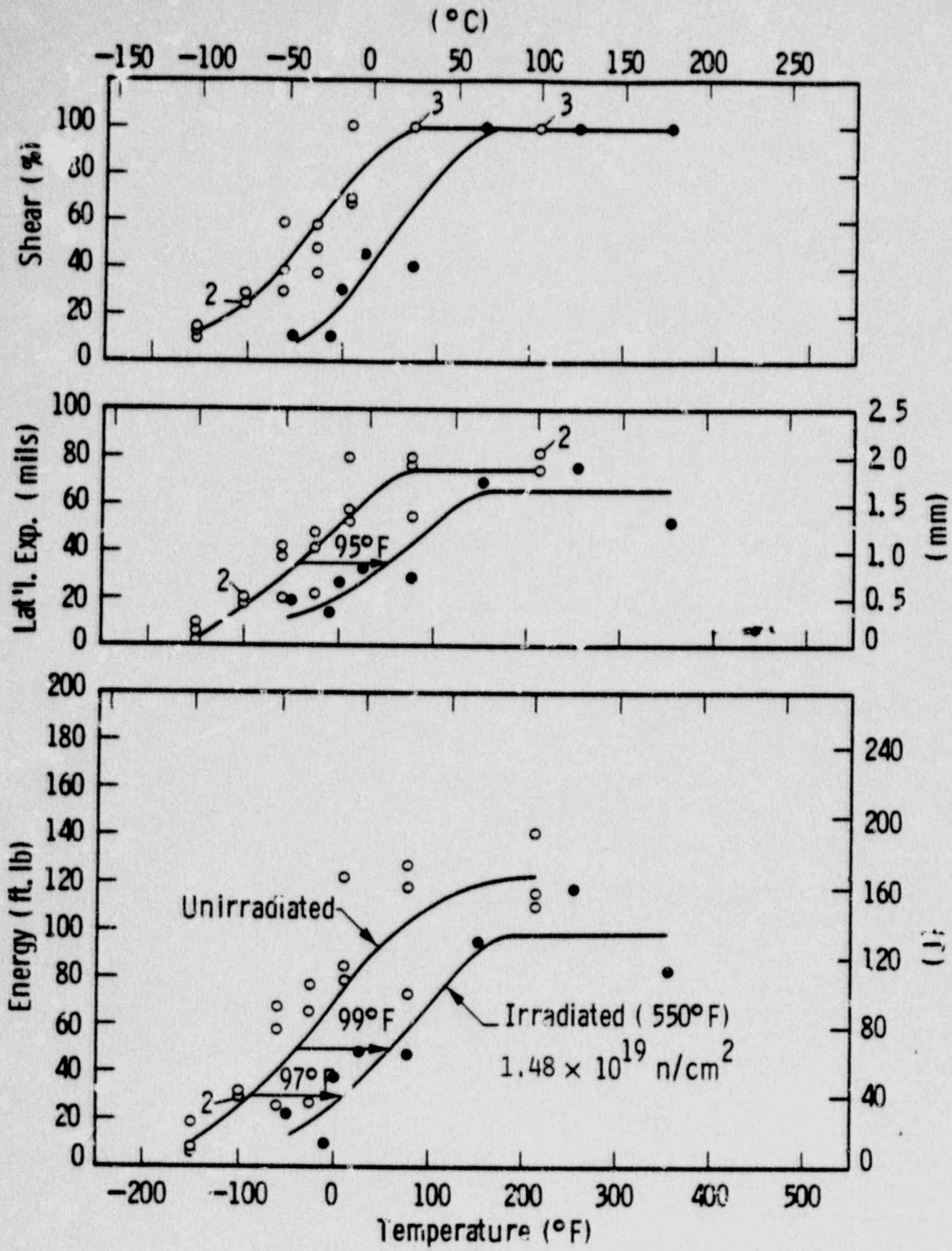

FIGURE 5-4 CHARPY V-NOTCH IMPACT DATA FOR ZION UNIT 2 REACTOR VESSEL WELD HEAT AFFECTED ZONE METAL

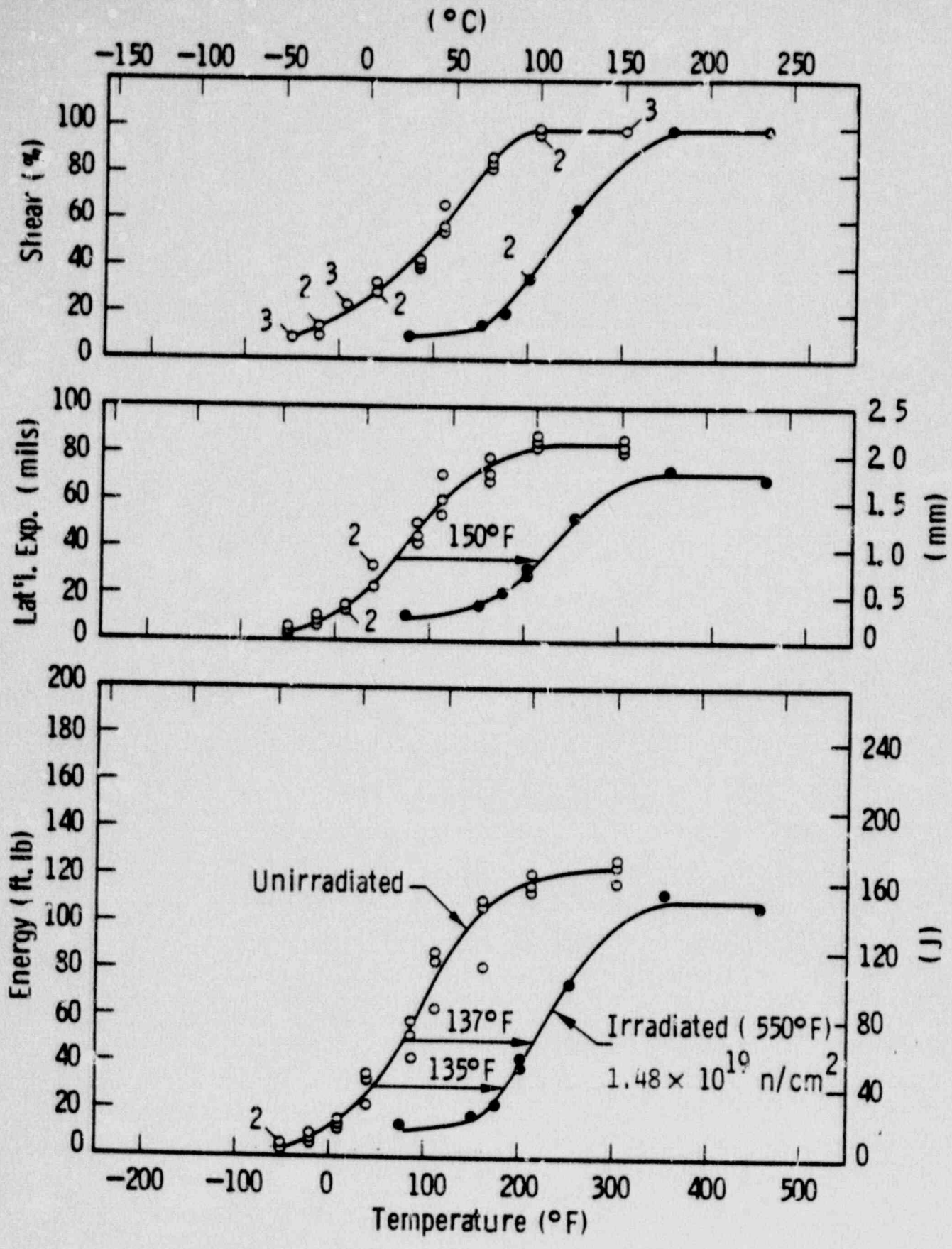

FIGURE 5-5 CHARPY V-NOTCH IMPACT DATA FOR ZION UNIT 2 A533 GRADE B CLASS 1 CORRELATION MONITOR MATERIAL (HSST PLATE 02)

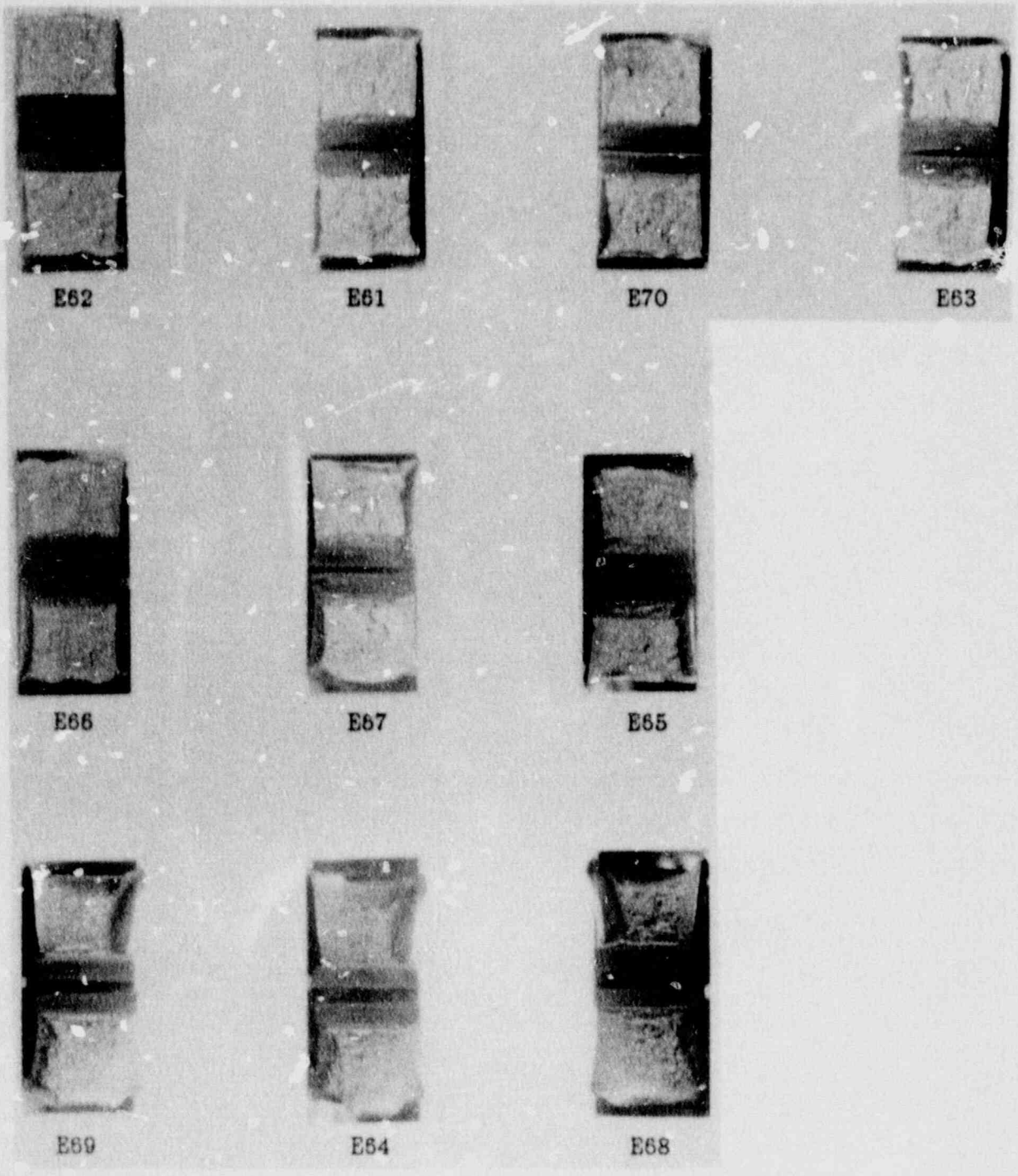

FIGURE 5-6 CHARPY IMPACT SPECIMEN FRACTURE SURFACES FOR ZION UNIT 2 REACTOR VESSEL SHELL PLATE C4007-1 (LONGITUDINAL ORIENTATION)

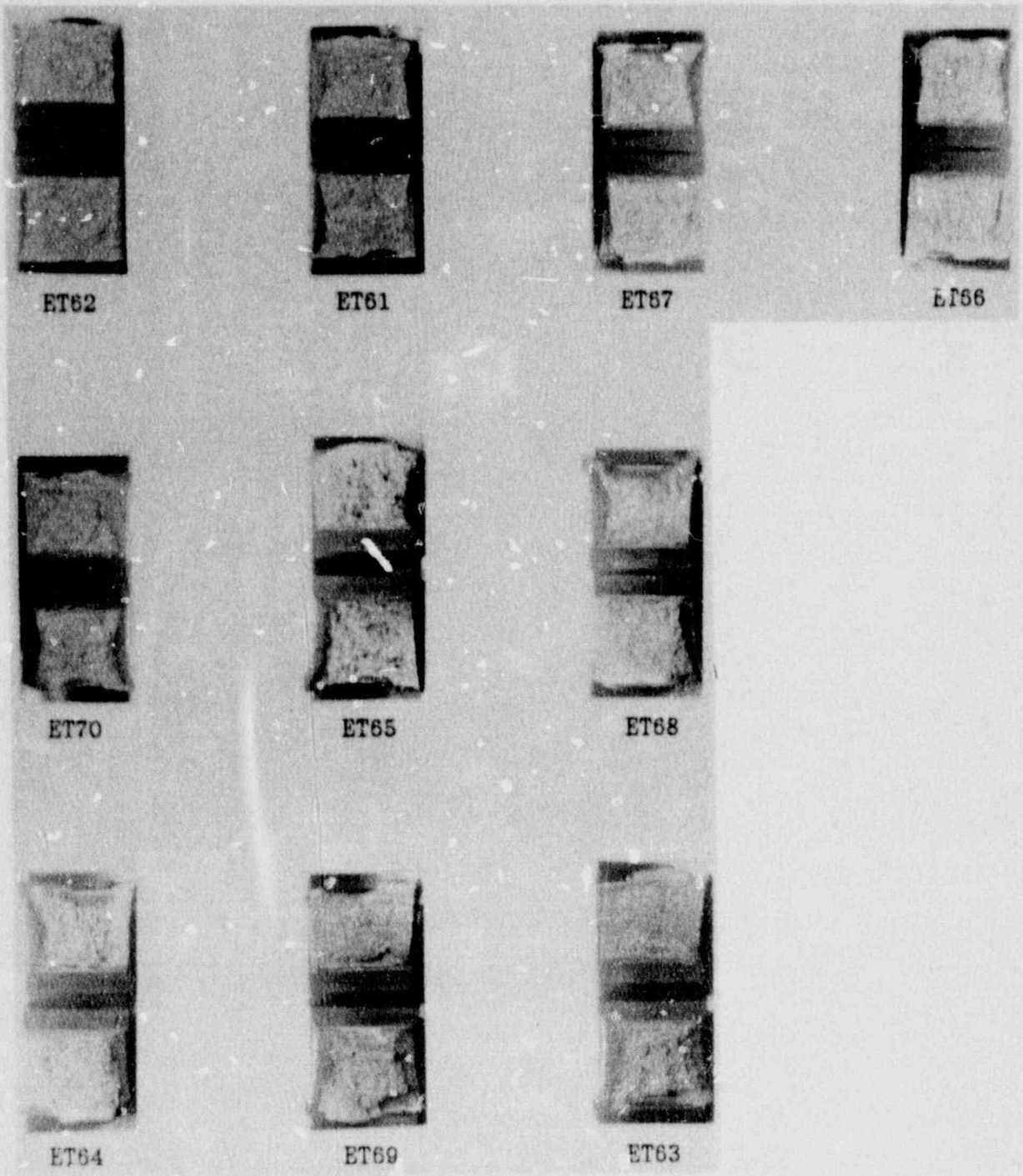

FIGURE 5-7 CHARPY IMPACT SPECIMEN FRACTURE SURFACES FOR ZION UNIT 2 REACTOR VESSEL SHELL PLATE C4007-1 (TRANSVERSE ORIENTATION)

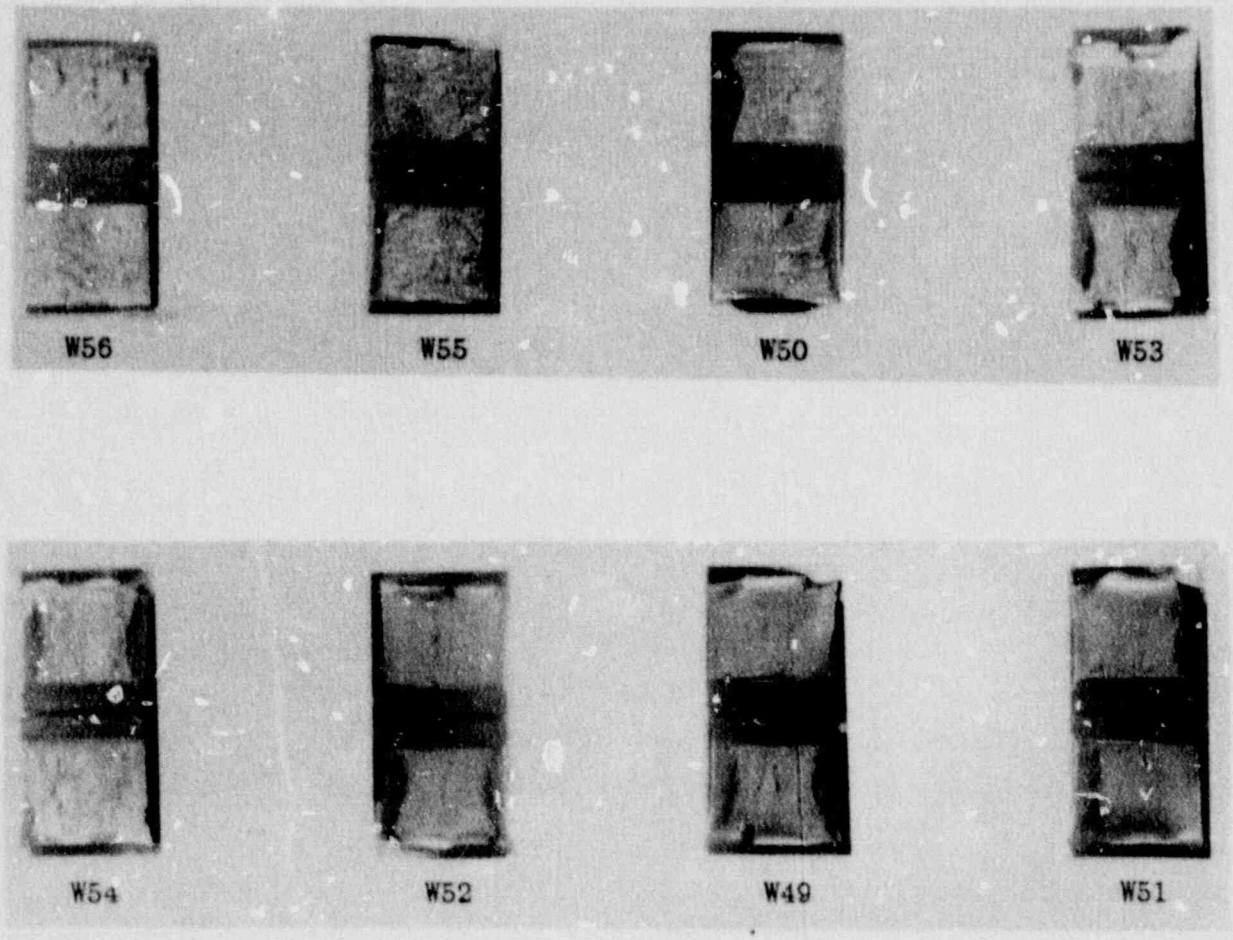

FIGURE 5 8 CHARPY IMPACT SPECIMEN FRACTURE SURFACES FOR ZION UNIT 2 REACTOR VESSEL WELD METAL

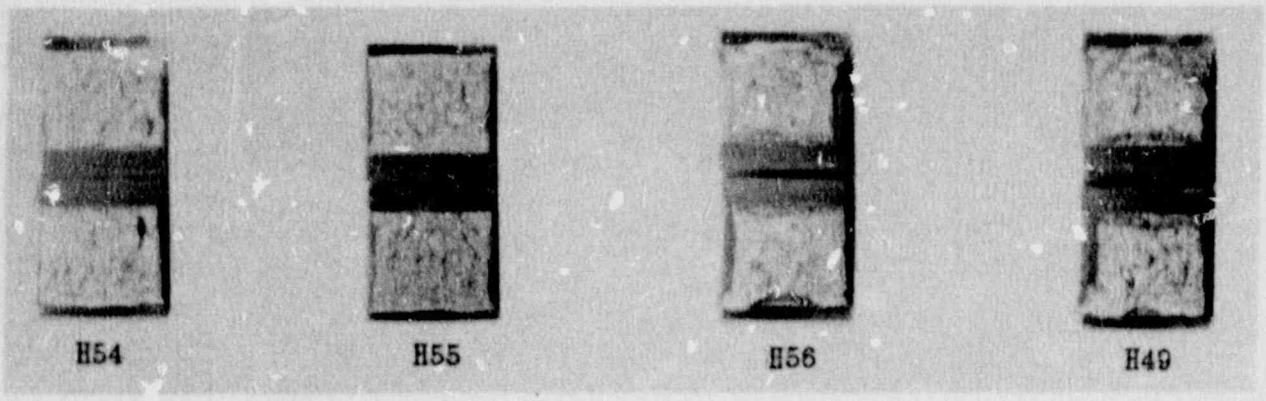

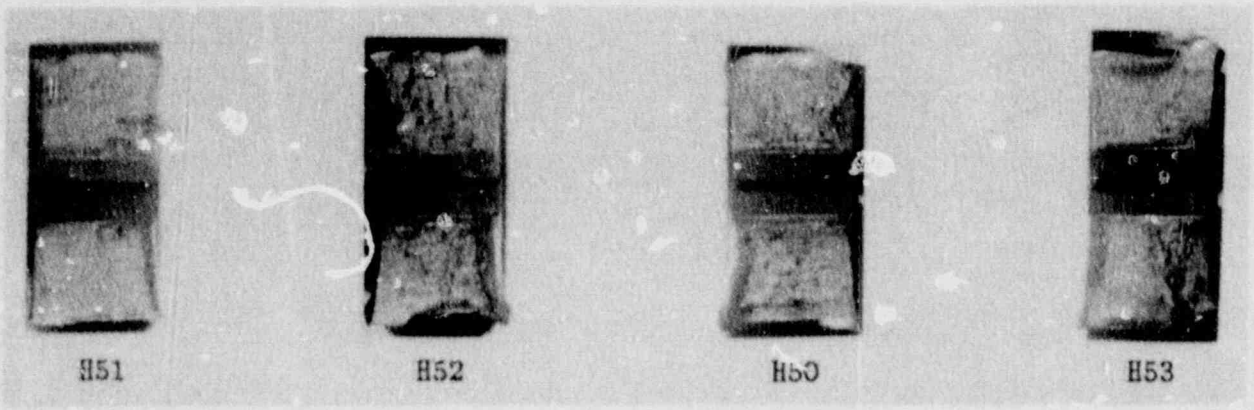

FIGURE 5-9 CHARPY IMPACT SPECIMEN FRACTURE SURFACES FOR ZION UNIT 2 REACTOR VESSEL WELD HAZ METAL

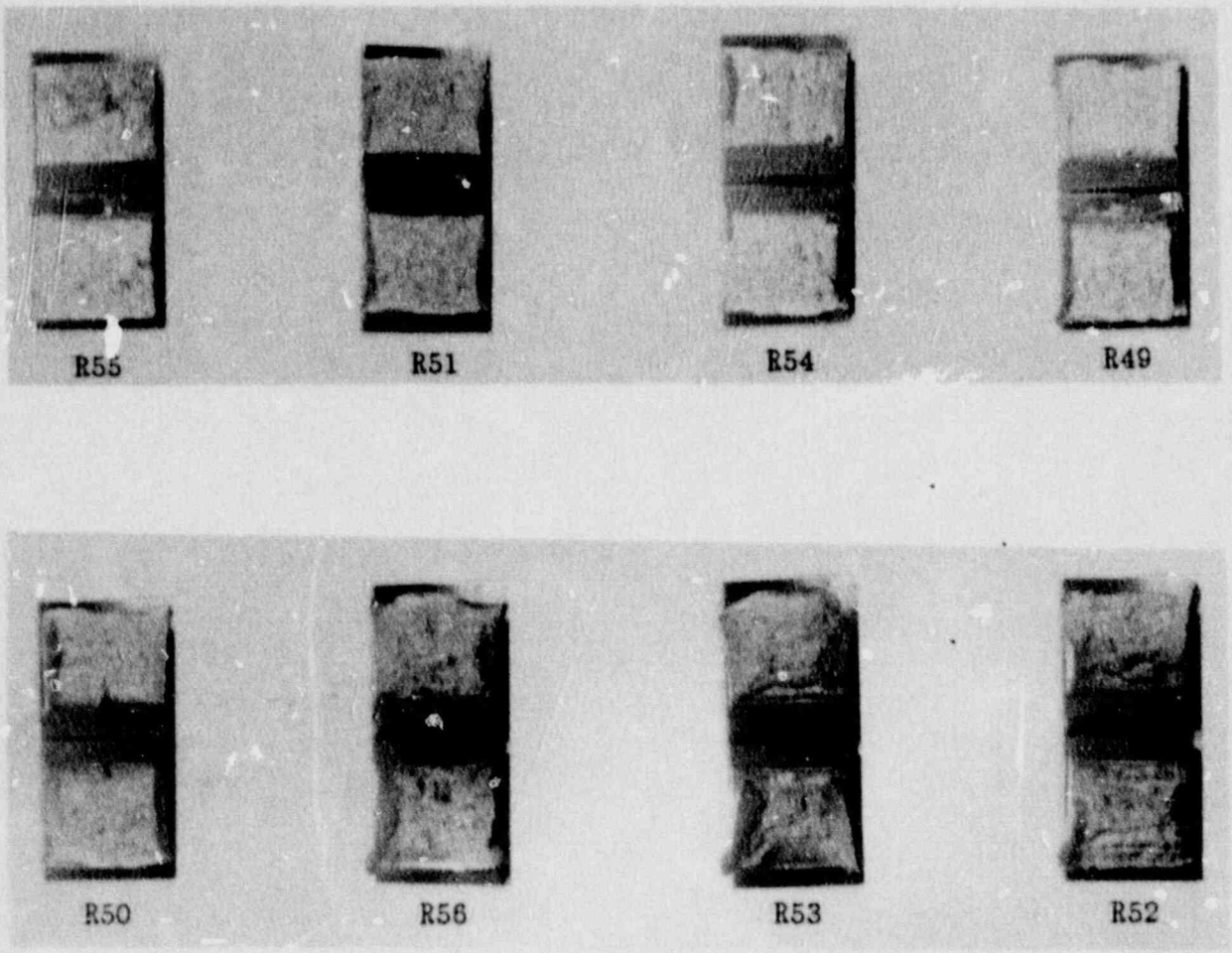

FIGURE 5-10 CHARPY IMPACT SPECIMEN FRACTURE SURFACES FOR ZION UNIT 2 ASTM CORRELATION MONITOR MATERIAL

1

IMAGE EVALUATION TEST TARGET (MT-3)

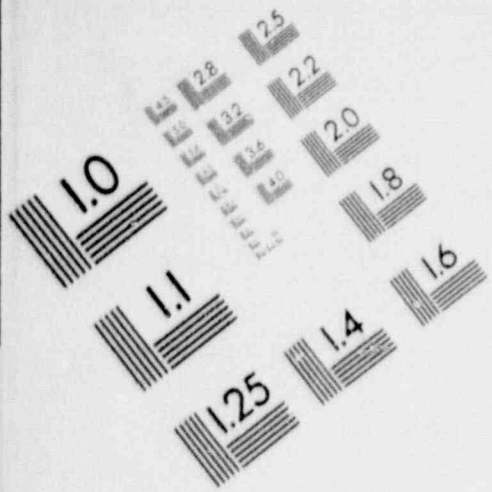

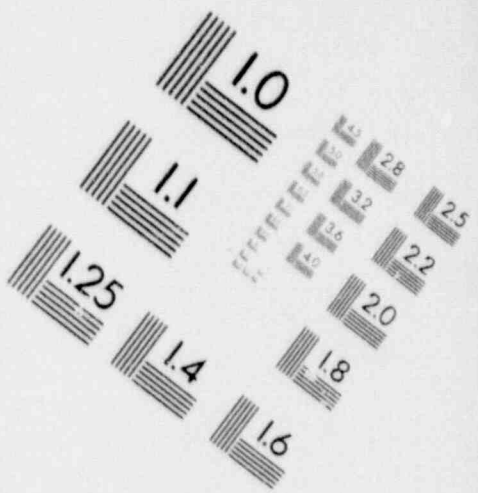

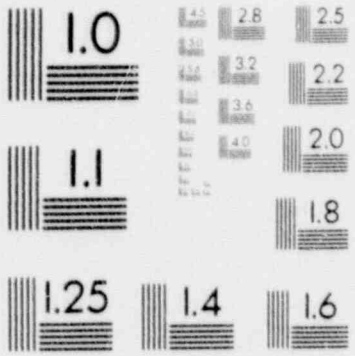

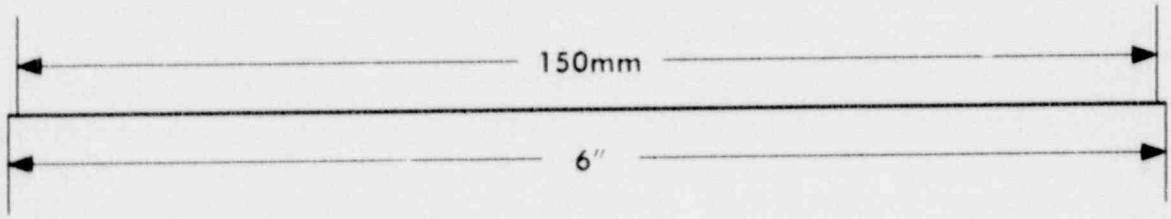

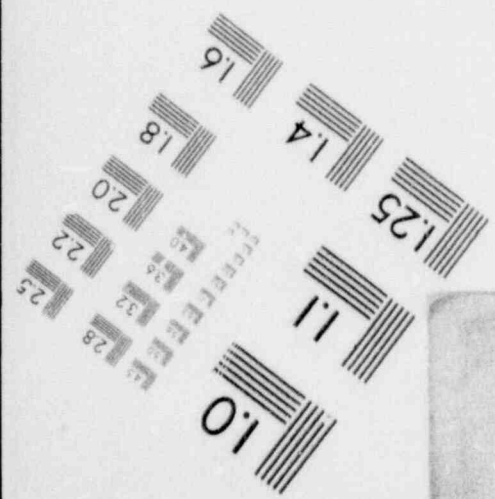

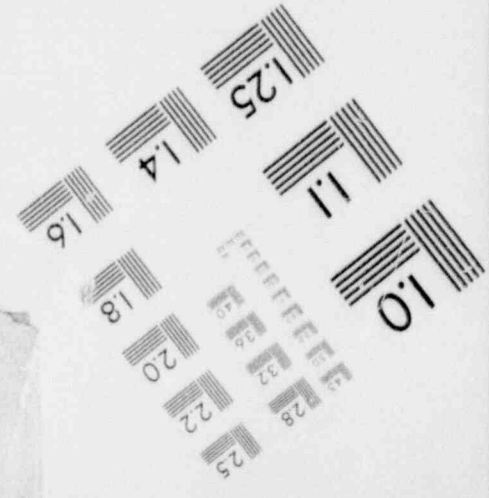

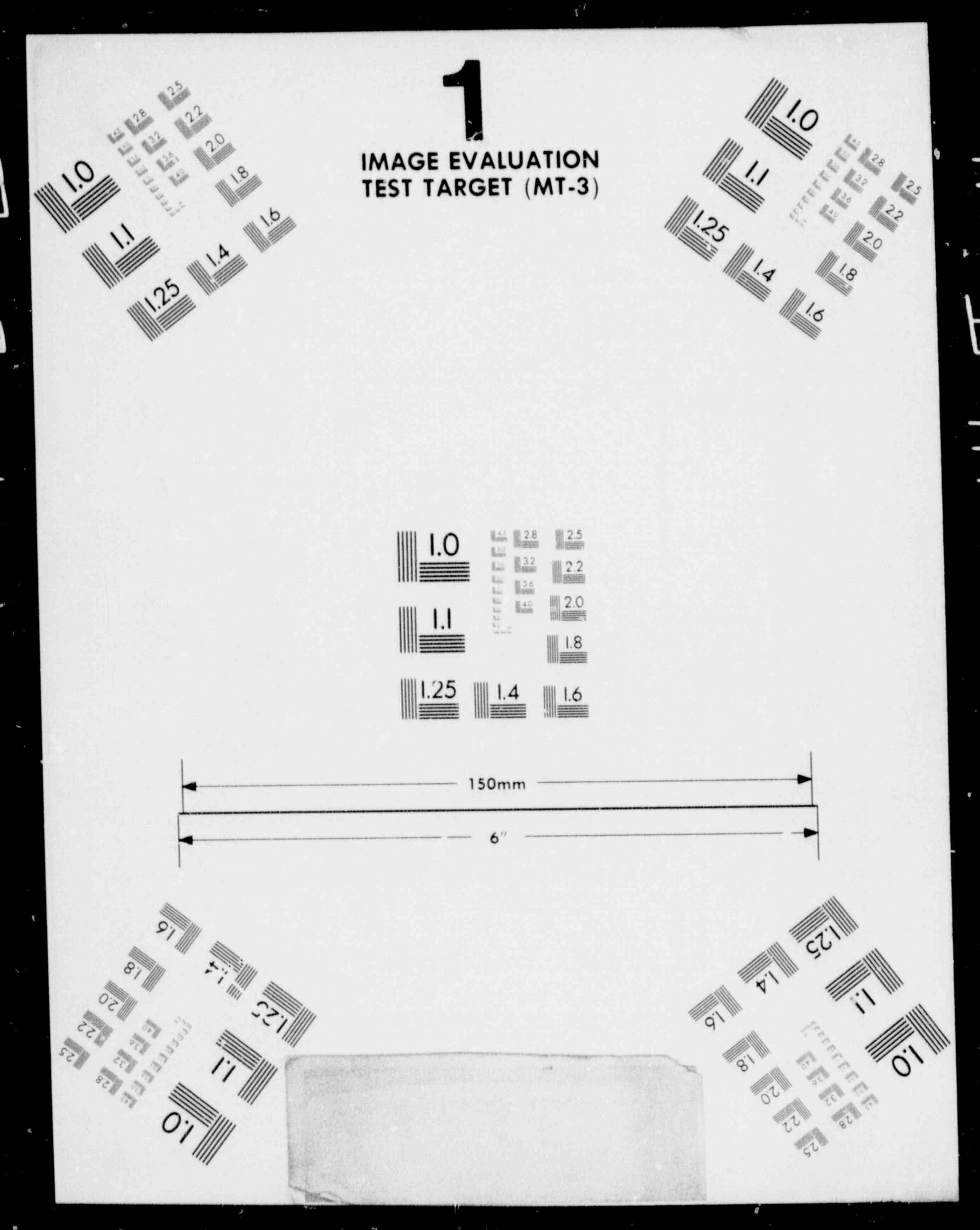
1
IMAGE EVALUATION
TEST TARGET (MT-3)
1.0
1.1
1.25
1.4
1.6
1.8
2.0
2.2
2.5
2.8
3.2
3.6
4.0
150mm
6"

1

IMAGE EVALUATION TEST TARGET (MT-3)

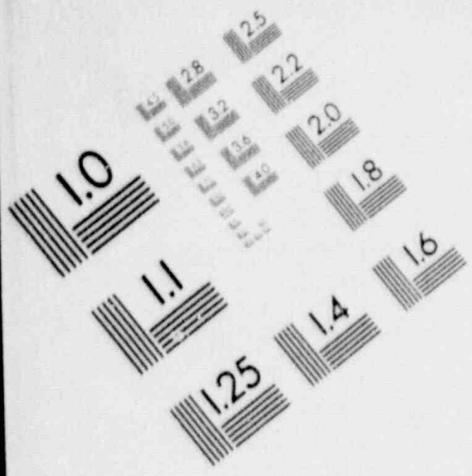

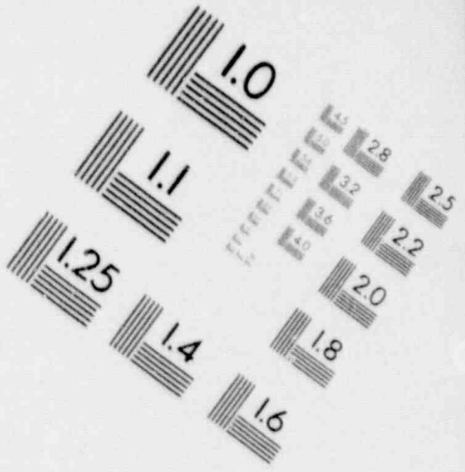

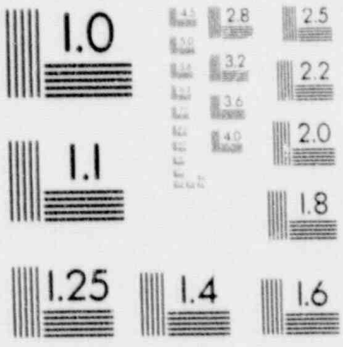

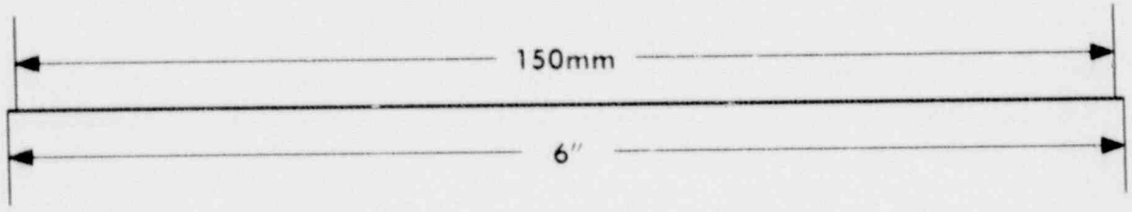

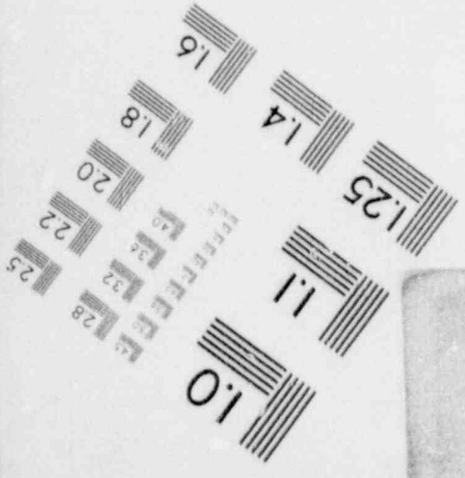

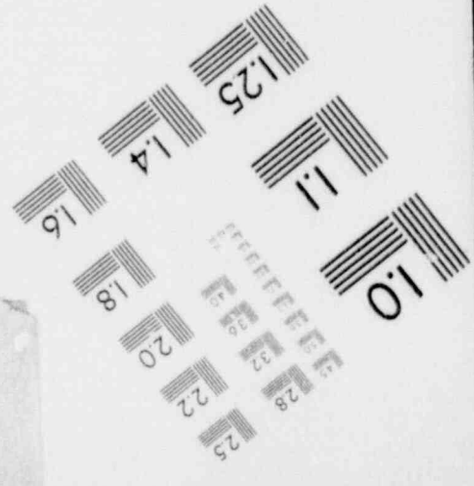

1

IMAGE EVALUATION TEST TARGET (MT-3)

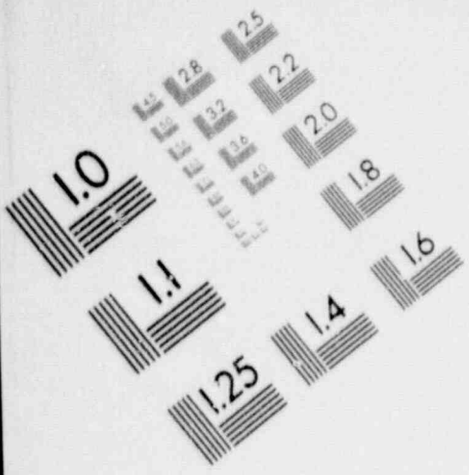

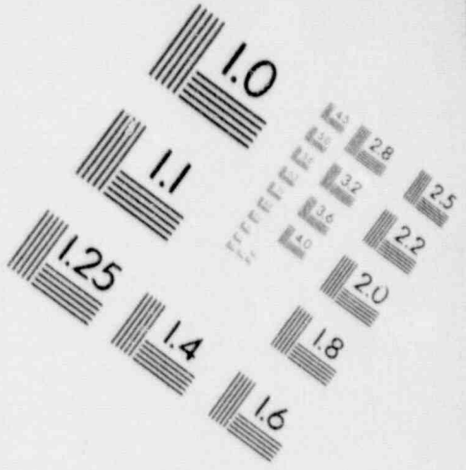

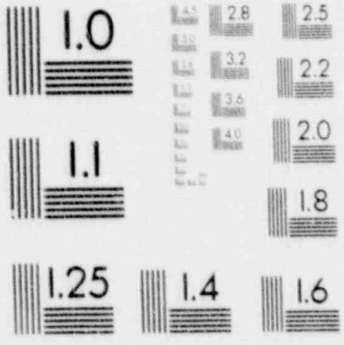

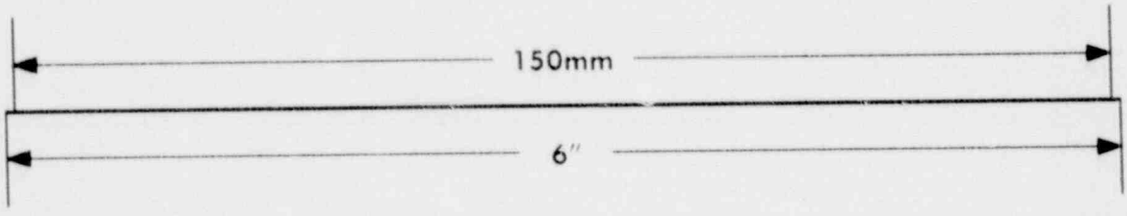

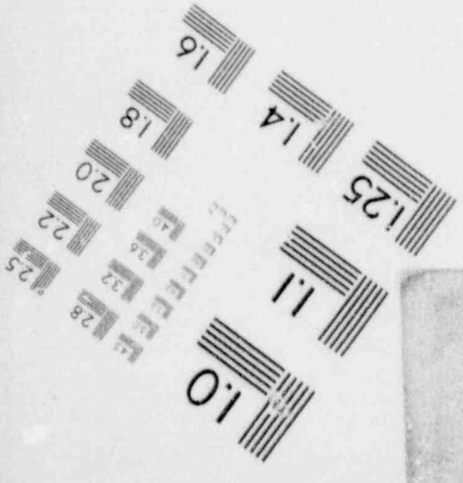

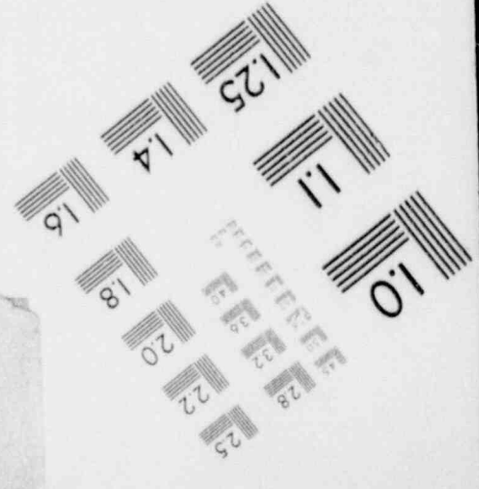

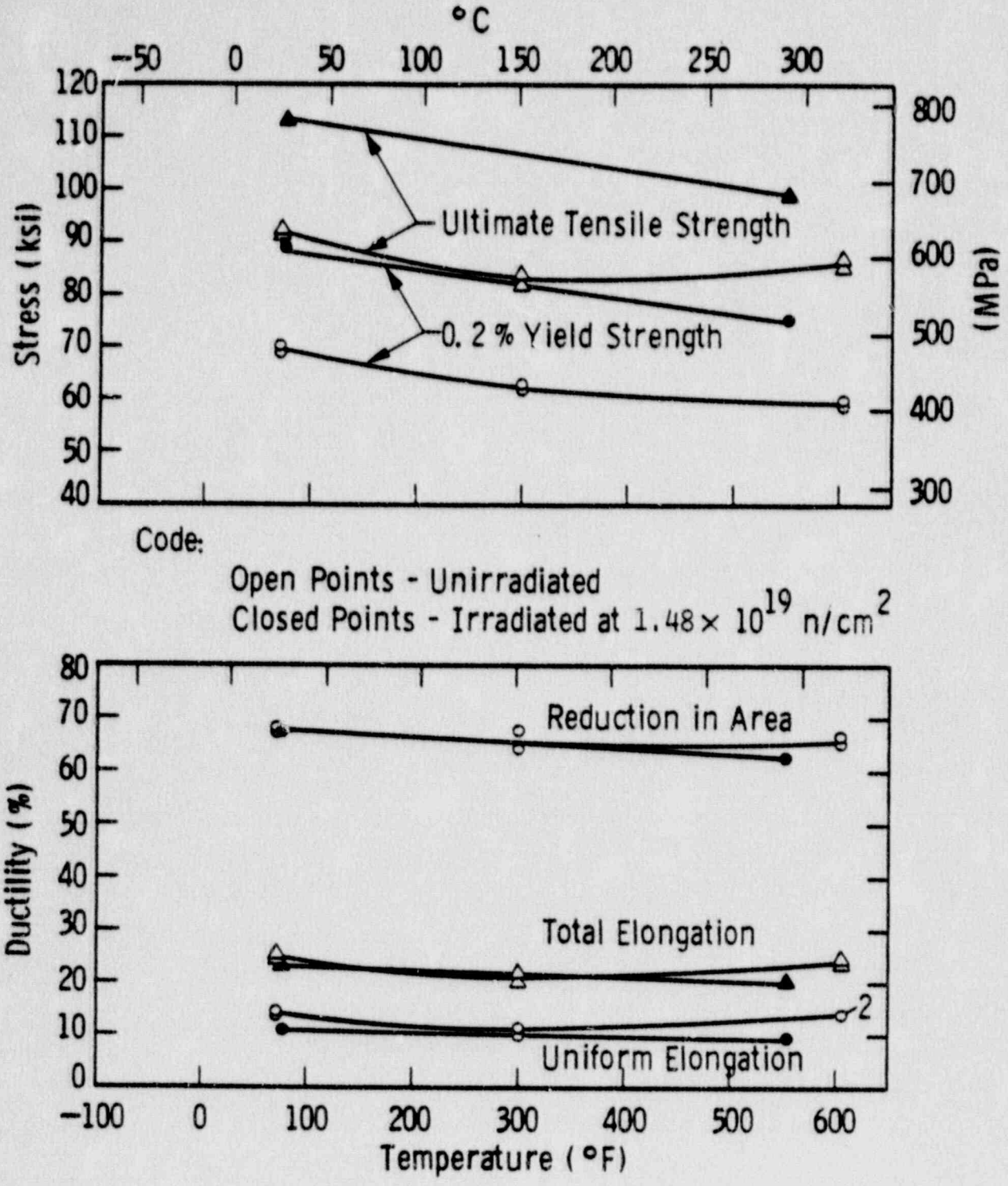

FIGURE 5-11 TENSILE PROPERTIES FOR ZION UNIT 2 REACTOR VESSEL SHELL PLATE C4007-1 (LONGITUDINAL ORIENTATION)

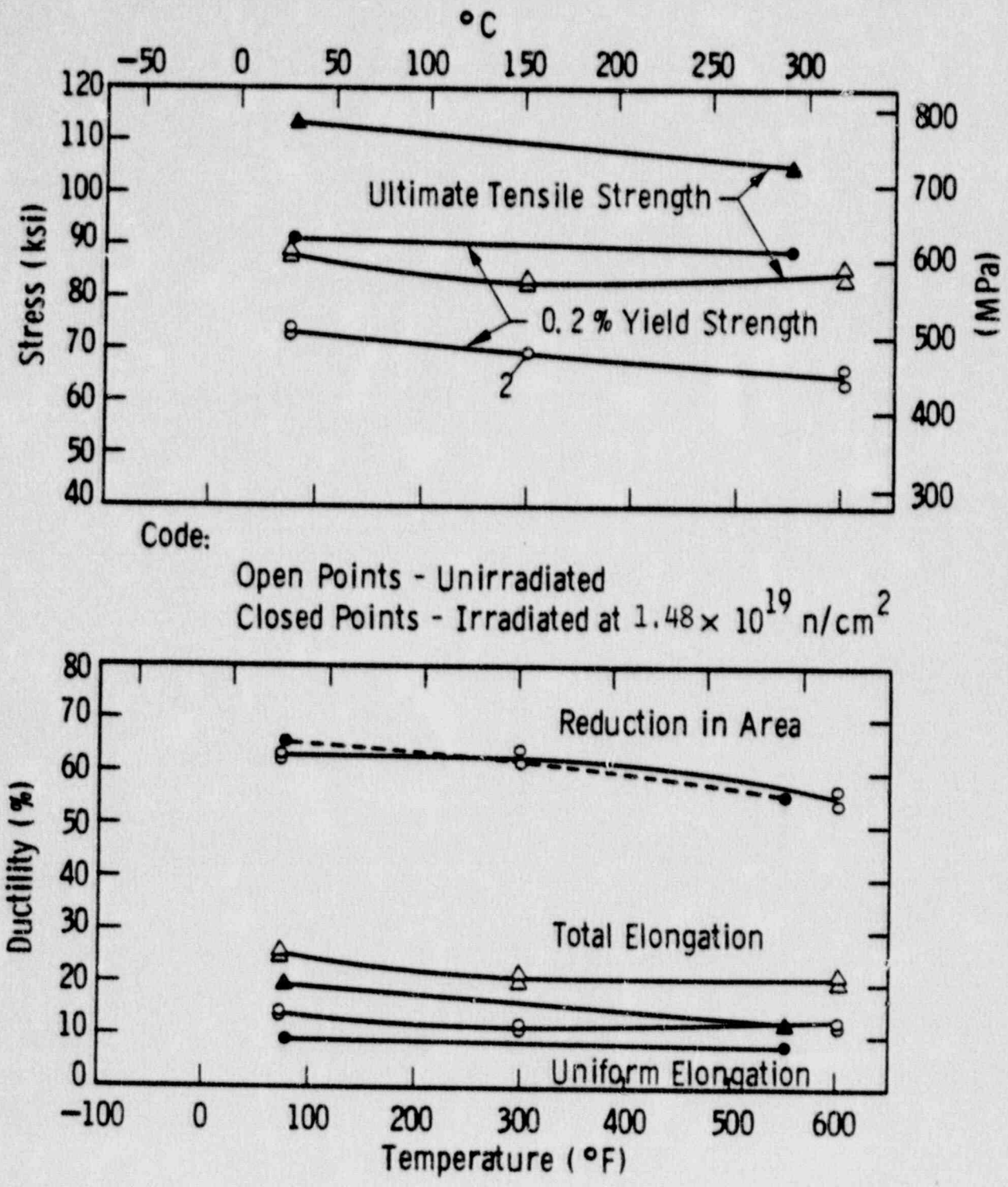

FIGURE 5-12 TENSILE PROPERTIES FOR ZION UNIT 2 REACTOR VESSEL WELD METAL

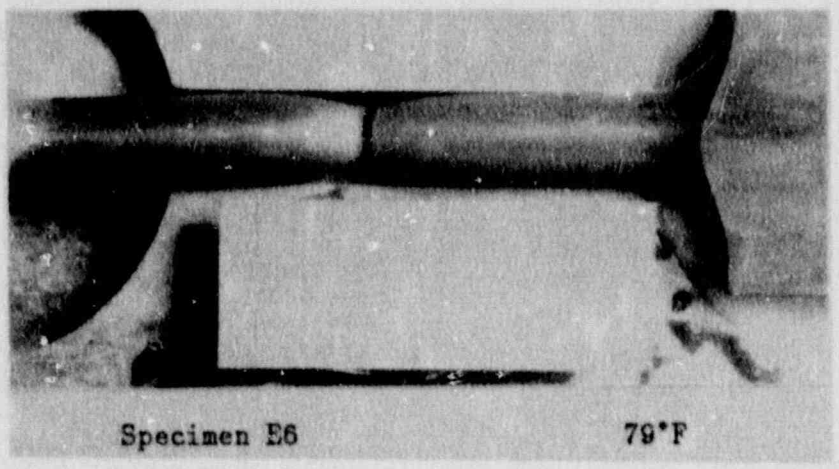

Specimen E6 79°F

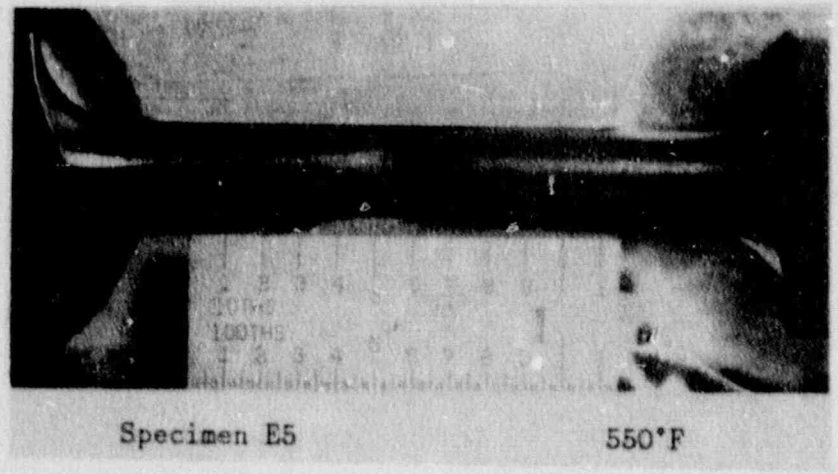

Specimen E5 550°F

FIGURE 5-13 FRACTURED TENSILE SPECIMENS FOR ZION UNIT 2 REACTOR VESSEL SHELL PLATE C4007-1 (LONGITUDINAL ORIENTATION)

Specimen W14 79°F

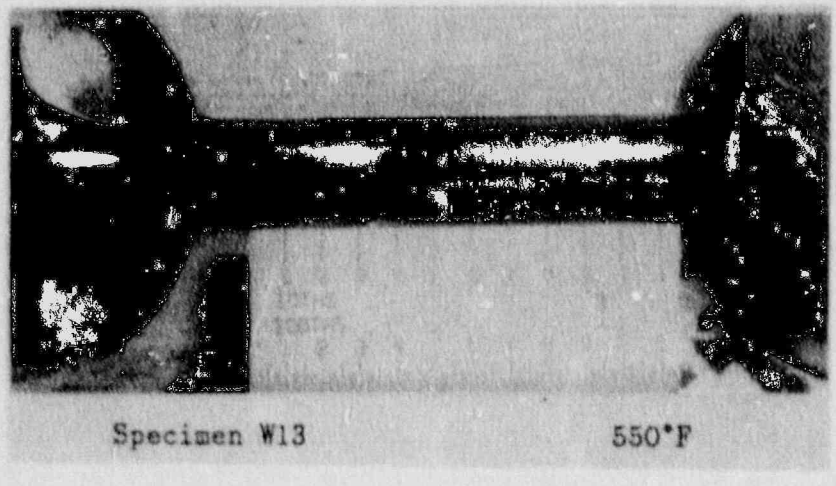

Specimen W13 550°F

FIGURE 5-14 FRACTURED TENSILE SPECIMENS FOR ZION UNIT 2 REACTOR VESSEL WELD METAL

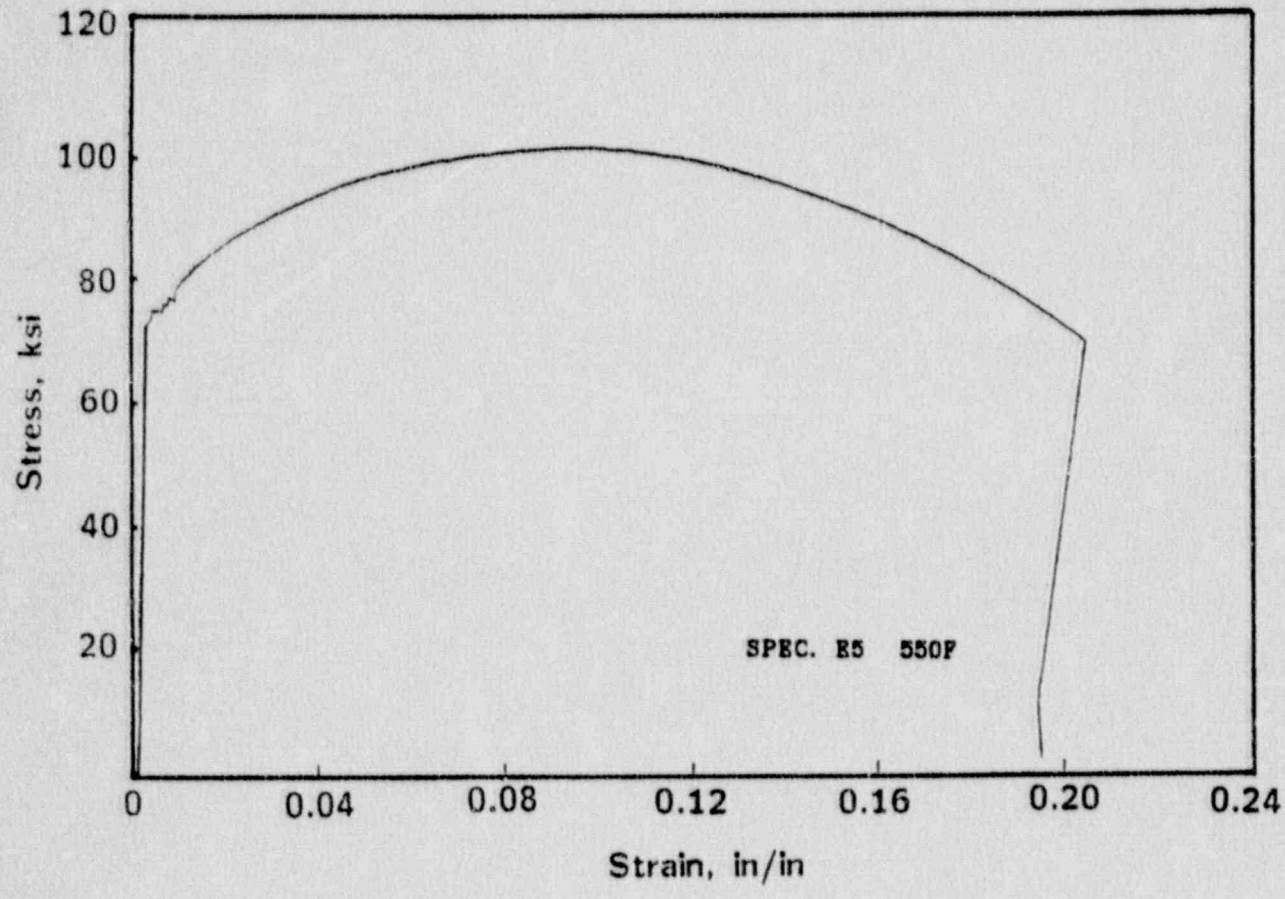

FIGURE 5-15 TYPICAL STRESS-STRAIN CURVE FOR TENSION SPECIMENS

6.0 RADIATION ANALYSIS AND NEUTRON DOSIMETRY

6.1 INTRODUCTION

Knowledge of the neutron environment within the reactor pressure vessel and surveillance capsule geometry is required as an integral part of LWR reactor pressure vessel surveillance programs for two reasons. First, in order to interpret the neutron radiation-induced material property changes observed in the test specimens, the neutron environment (energy spectrum, flux, fluence) to which the test specimens were exposed must be known. Second, in order to relate the changes observed in the test specimens to the present and future condition of the reactor vessel, a relationship must be established between the neutron environment at various positions within the reactor vessel and that experienced by the test specimens. The former requirement is normally met by employing a combination of rigorous analytical techniques and measurements obtained with passive neutron flux monitors contained in each of the surveillance capsules. The latter information is derived solely from analysis.

The use of fast neutron fluence (E > 1.0 MeV) to correlate measured materials properties changes to the neutron exposure of the material for light water reactor applications has traditionally been accepted for development of damage trend curves as well as for the implementation of trend curve data to assess vessel condition. In recent years, however, it has been suggested that an exposure model that accounts for differences in neutron energy spectra between surveillance capsule locations and positions within the vessel wall could lead to an improvement in the uncertainties associated with damage trend curves as well as to a more accurate evaluation of damage gradients through the pressure vessel wall.

Because of this potential shift away from a threshold fluence toward an energy dependent damage function for data correlation, ASTM Standard Practice E853, "Analysis and Interpretation of Light Water Reactor Surveillance Results," recommends reporting displacements per iron atom (dpa) along with fluence

(E > 1.0 MeV) to provide a data base for future reference. The energy dependent dpa function to be used for this evaluation is specified in ASTM Standard Practice E693, "Characterizing Neutron Exposures in Ferritic Steels in Terms of Displacements per Atom." The application of the dpa parameter to the assessment of embrittlement gradients through the thickness of the pressure vessel wall has already been promulgated in Revision 2 to the Regulatory Guide 1.99, "Radiation Damage to Reactor Vessel Materials."

This section provides the results of the neutron dosimetry evaluations performed in conjunction with the analysis of test specimens contained in surveillance Capsule Y. Updated evaluations of dosimetry from prior surveillance capsule withdrawals are also presented to provide a complete data base for use in establishing the integrated exposure of the pressure vessel wall. These re-evaluations include data from Capsules U and T withdrawn at the conclusion of the first and fourth fuel cycles, respectively.

Fast neutron exposure parameters in terms of fast neutrons fluence (E > 1.0 Mev), fast neutron fluence (E > 0.1 Mev), and iron atom displacements (dpa) are established for the irradiation history. The analytical formalism relating the measured capsule exposures to the exposure of the vessel wall is described and used to project the integrated exposure of the vessel itself. Also, uncertainties associated with the derived exposure parameters are provided.

6.2 DISCRETE ORDINATES ANALYSIS

A plan view of the reactor geometry at the core midplane is shown in Figure 4-1. Eight irradiation capsules attached to the thermal shield are included in the reactor design to constitute the reactor vessel surveillance program. Four capsules are located symetrically at azimuthal angles of 4° and 40° relative to the core cardinal axis as shown in Figure 4-1.

A plan view of a surveillance capsule holder attached to the thermal shield is shown in Figure 6-1. The stainless steel specimen containers are 1-inch square and approximately 38 inches in height. The containers are positioned

axially such that the specimens are centered on the core midplane, thus spanning the central 3 feet of the 12-foot high reactor core.

From a neutron transport standpoint, the surveillance capsule structures are significant. They have a marked effect on both the distribution of neutron flux and the neutron energy spectrum in the water annulus between the thermal shield and the reactor vessel. In order to properly determine the neutron environment at the test specimen locations, the capsules themselves must be included in the analytical model.

In performing the fast neutron exposure evaluations for the surveillance capsules and reactor vessel, two distinct sets of transport calculations were carried out. The first, a single computation in the conventional forward mode, was used primarily to obtain relative neutron energy distributions throughout the reactor geometry as well as to establish relative radial distributions of exposure parameters {ϕ(E > 1.0 Mev,) ϕ(E > 0.1 Mev), and dpa} through the vessel wall. The neutron spectral information was required for the interpretation of neutron dosimetry withdrawn from the surveillance capsule as well as for the determination of exposure parameter ratios; i.e., dpa/ϕ(E > 1.0 MeV), within the pressure vessel geometry. The relative radial gradient information was required to permit the projection of measured exposure parameters to locations interior to the pressure vessel wall; i.e., the 1/4T, 1/2T, and 3/4T locations.

The second set of calculations consisted of a series of adjoint analyses relating the fast neutron flux (E > 1.0 MeV) at surveillance capsule positions, and several azimuthal locations on the pressure vessel inner radius to neutron source distributions within the reactor core. The importance functions generated from these adjoint analyses provided the basis for all absolute exposure projections and comparison with measurement. These importance functions, when combined with cycle specific neutron source distributions, yielded absolute predictions of neutron exposure at the locations of interest for the first 10 cycles of irradiation; and established the means to perform similar predictions and dosimetry evaluations for all subsequent fuel cycles. It is important to note that the cycle specific neutron source distributions utilized in these analyses included not only

spatial variations of fission rates within the reactor core; but, also accounted for the effects of varying neutron yield per fission and fission spectrum introduced by the build-up of plutonium as the burnup of individual fuel assemblies increased.

The absolute cycle specific data from the adjoint evaluations together with relative neutron energy spectra and radial distribution information from the forward calculation provided the means to:

1. Evaluate neutron dosimetry obtained from surveillance capsule locations.

2. Extrapolate dosimetry results to key locations at the inner radius and through the thickness of the pressure vessel wall.

3. Enable a direct comparison of analytical prediction with measurement.

4. Establish a mechanism for projection of pressure vessel exposure as the design of each new fuel cycle evolves.

The forward transport calculation for the reactor model summarized in Figures 4-1 and 6-1 was carried out in R, θ geometry using the DOT two-dimensional discrete ordinates code [6] and the SAILOR cross-section library [7]. The SAILOR library is a 47 group ENDFB-IV based data set produced specifically for light water reactor applications. In these analyses anisotopic scattering was treated with a P_3 expansion of the cross-sections and the angular discretization was modeled with an S_8 order of angular quadrature.

The reference core power distribution utilized in the forward analysis was derived from statistical studies of long-term operation of Westinghouse 4-loop plants. Inherent in the development of this reference core power distribution is the use of an out-in fuel management strategy; i.e., fresh fuel on the core periphery. Furthermore, for the peripheral fuel assemblies, a 2σ uncertainty derived from the statistical evaluation of plant to plant and cycle to cycle variations in peripheral power was used. Since it is unlikely

that a single reactor would have a power distribution at the nominal +2σ level for a large number of fuel cycles, the use of this reference distribution is expected to yield somewhat conservative results.

All adjoint analyses were also carried out using an S_8 order of angular quadrature and the P_3 cross-section approximation from the SAILOR library. Adjoint source locations were chosen at several azimuthal locations along the pressure vessel inner radius as well as the geometric center of each surveillance capsule. Again, these calculations were run in R, Θ geometry to provide neutron source distribution importance functions for the exposure parameter of interest; in this case, ϕ (E > 1.0 MeV). Having the importance functions and appropriate core source distributions, the response of interest could be calculated as:

$$R(r, \theta) = \int_r \int_\theta \int_E I(r, \theta, E)\, S(r, \theta, E)\, r\, dr\, d\theta\, dE$$

where: $R(r, \theta)$ = ϕ (E > 1.0 MeV) at radius r and azimuthal angle Θ

$I(r, \theta, E)$ = Adjoint importance function at radius, r, azimuthal angle Θ, and neutron source energy E.

$S(r, \theta, E)$ = Neutron source strength at core location r, Θ and energy E.

Although the adjoint importance functions used in the Zion Unit 2 analysis were based on a response function defined by the threshold neutron flux (E > 1.0 MeV), prior calculations have shown that, while the implementation of low leakage loading patterns significantly impact the magnitude and the spatial distribution of the neutron field, changes in the relative neutron energy spectrum are of second order. Thus, for a given location the ratio of dpa/ϕ (E > 1.0 MeV) is insensitive to changing core source distributions. In the application of these adjoint important functions to the Zion Unit 2 reactor, therefore, calculation of the iron displacement rates (dpa) and the neutron flux (E > 0.1 MeV) were computed on a cycle specific basis by using dpa/ϕ (E > 1.0 MeV) and ϕ (E > 0.1 MeV)/ϕ (E > 1.0 MeV) ratios from the forward analysis in conjunction with the cycle specific ϕ (E > 1.0 MeV) solutions from the individual adjoint evaluations.

The reactor core power distributions used in the plant specific adjoint calculations were taken from the fuel cycle design reports for the first ten operating cycles of Zion Unit 2 [8 thru 17].

Selected results from the neutron transport analyses performed for the Zion Unit 2 reactor are provided in Tables 6-1 through 6-5. The data listed in these tables establish the means for absolute comparisons of analysis and measurement for the capsule irradiation period and provide the means to correlate dosimetry results with the corresponding neutron exposure of the pressure vessel wall.

In Table 6-1, the calculated exposure parameters {ϕ (E > 1.0 MeV), ϕ (E > 0.1 MeV), and dpa} are given at the geometric center of the two surveillance capsule positions for both the design basis and the plant specific core power distributions. The plant specific data, based on the adjoint transport analysis, are meant to establish the absolute comparison of measurement with analysis. The design basis data derived from the forward calculation are provided as a point of reference against which plant specific fluence evaluations can be compared. Similar data is given in Table 6-2 for the pressure vessel inner radius. Again, the three pertinent exposure parameters are listed for both the design basis and the cycle 1 through 10 average plant specific power distributions. It is important to note that the data for the vessel inner radius were taken at the clad/base metal interface; and, thus, represent the maximum exposure levels of the vessel wall itself.

Radial gradient information for neutron flux (E > 1.0 MeV), neutron flux (E > 0.1 MeV), and iron atom displacement rate is given in Tables 6-3, 6-4, and 6-5, respectively. The data, obtained from the forward neutron transport calculation, are presented on a relative basis for each exposure parameter at several azimuthal locations. Exposure parameter distributions within the wall may be obtained by normalizing the calculated or projected exposure at the vessel inner radius to the gradient data given in Tables 6-3 through 6-5.

For example, the neutron flux (E > 1.0 MeV) at the 1/4T position on the 45° azimuth is given by:

$$\phi_{1/4T}(45°) = \phi(220.27, 45°)\ F\ (225.75, 45°)$$

where $\phi_{1/4T}(45°)$ = Projected neutron flux at the 1/4T position on the 45° azimuth

$\phi\ (220.27, 45°)$ = Projected or calculated neutron flux at the vessel inner radius on the 45° azimuth.

F (225.75, 45°) = Relative radial distribution function from Table 6-3.

Similar expressions apply for exposure parameters in terms of ϕ(E > 0.1 MeV) and dpa/sec.

6.3 NEUTRON DOSIMETRY

The passive neutron sensors included in the Zion Unit 2 surveillance program are listed in Table 6-6. Also given in Table 6-6 are the primary nuclear reactions and associated nuclear constants that were used in the evaluation of the neutron energy spectrum within the capsule and the subsequent determination of the various exposure parameters of interest {ϕ (E > 1.0 Mev), ϕ (E > 0.1 MeV), dpa}.

The relative locations of the neutron sensors within the capsules are shown in Figure 4-2. The iron, nickel, copper, and cobalt-aluminum monitors, in wire form, were placed in holes drilled in spacers at several axial levels within the capsules. The cadmium-shielded neptunium and uranium fission monitors were accommodated within the dosimeter block located near the center of the capsule.

The use of passive monitors such as those listed in Table 6-6 does not yield a direct measure of the energy dependent flux level at the point of interest.

Rather, the activation or fission process is a measure of the integrated effect that the time- and energy-dependent neutron flux has on the target material over the course of the irradiation period. An accurate assessment of the average neutron flux level incident on the various monitors may be derived from the activation measurements only if the irradiation parameters are well known. In particular, the following variables are of interest:

- o The specific activity of each monitor.
- o The operating history of the reactor.
- o The energy response of the monitor.
- o The neutron energy spectrum at the monitor location.
- o The physical characteristics of the monitor.

The specific activity of each of the neutron monitors was determined using established ASTM procedures [18 through 31]. Following sample preparation and weighing, the activity of each monitor was determined by means of a lithium-drifted germanium, Ge(Li), gamma spectrometer. The irradiation history of the Zion Unit 2 reactor during cycles 1 through 10 was obtained from NUREG-0020, "Licensed Operating Reactors Status Summary Report" for the applicable period.

The irradiation history applicable to capsule Y is given in Table 6-7. Measured and saturated reaction product specific activities as well as measured full power reaction rates are listed in Table 6-8. Reaction rate values were derived using the pertinent data from Tables 6-6 and 6-7.

Values of key fast neutron exposure parameters were derived from the measured reaction rates using the FERRET least squares adjustment code [32]. The FERRET approach used the measured reaction rate data and the calculated neutron energy spectrum at the the center of the surveillance capsule as input and proceeded to adjust a priori (calculated) group fluxes to produce a best fit (in a least squares sense) to the reaction rate data. The exposure parameters along with associated uncertainties where then obtained from the adjusted spectra.

In the FERRET evaluations, a log normal least-squares algorithm weights both the a priori values and the measured data in accordance with the assigned uncertainties and correlations. In general, the measured values f are linearly related to the flux ϕ by some response matrix A:

$$f_i^{(s,\alpha)} = \sum_g A_{ig}^{(s)} \phi_g^{(\alpha)}$$

where i indexes the measured values belonging to a single data set s, g designates the energy group and α delineates spectra that may be simultaneously adjusted. For example,

$$R_i = \sum_g \sigma_{ig} \phi_g$$

relates a set of measured reaction rates R_i to a single spectrum ϕ_g by the multigroup cross section σ_{ig}. (In this case, FERRET also adjusts the cross-sections.) The lognormal approach automatically accounts for the physical constraint of positive fluxes, even with the large assigned uncertainties.

In the FERRET analysis of the dosimetry data, the continuous quantities (i.e., fluxes and cross-sections) were approximated in 53 groups. The calculated fluxes from the discrete ordinates analysis were expanded into the FERRET group structure using the SAND-II code [33]. This procedure was carried out by first expanding the a priori spectrum into the SAND-II 620 group structure using a SPLINE interpolation procedure for interpolation in regions where group boundaries do not coincide. The 620-point spectrum was then easily collapsed to the group scheme used in FERRET.

The cross-sections were also collapsed into the 53 energy-group structure using SAND II with calculated spectra (as expanded to 620 groups) as weighting functions. The cross sections were taken from the ENDF/B-V dosimetry file. Uncertainty estimates and 53 x 53 covariance matrices were constructed for each cross section. Correlations between cross sections were neglected due to data and code limitations, but are expected to be unimportant.

For each set of data or a priori values, the inverse of the corresponding relative covariance matrix M is used as a statistical weight. In some cases, as for the cross sections, a multigroup covariance matrix is used. More often, a simple parameterized form is used:

$$M_{gg'} = R_N^2 + R_g R_{g'} P_{gg'}$$

where R_N specifies an overall fractional normalization uncertainty (i.e., complete correlation) for the corresponding set of values. The fractional uncertainties R_g specify additional random uncertainties for group g that are correlated with a correlation matrix:

$$P_{gg'} = (1 - \theta)\, \delta_{gg'} + \theta \exp\left[-\frac{(g-g')^2}{2\gamma^2}\right]$$

The first term specifies purely random uncertainties while the second term describes short-range correlations over a range γ (θ specifies the strength of the latter term.)

For the a priori calculated fluxes, a short-range correlation of $\gamma = 6$ groups was used. This choice implies that neighboring groups are strongly correlated when θ is close to 1. Strong long-range correlations (or anticorrelations) were justified based on information presented by R. E. Maerker [34]. Maerker's results are closely duplicated when $\gamma = 6$. For the integral reaction rate covariances, simple normalization and random uncertainties were combined as deduced from experimental uncertainties.

Results of the FERRET evaluation of the capsule Y dosimetry are given in Table 6-9 The data summarized in Table 6-9 indicated that the capsule received an integrated exposure of 1.48×10^{19} n/cm^2 (E > 1.0 MeV) with an associated uncertainty of ± 8%. Also reported are capsule exposures in terms of fluence (E > 0.1 MeV) and iron atom displacements (dpa). Summaries of the fit of the adjusted spectrum are provided in Table 6-10. In general, excellent results were achieved in the fits of the adjusted spectrum to the individual experimental reaction rates. The adjusted spectrum itself is tabulated in Table 6-11 for the FERRET 53 energy group structure.

A summary of the measured and calculated neutron exposure of capsule Y is presented in Table 6-12 along with the updated exposure evaluations for capsules T and U. This information is also shown graphically as a function of reactor full power operating time in Figure 6-2. The agreement between calculation and measurement is good for all exposure parameters in each of the capsules withdrawn to date. The measured data from the early capsules (T and U) exceed prediction by approximately 14%, whereas, the data from capsule Y falls roughly 7% below prediction. In general, the measured data tracks the predicted exposure at the capsule locations quite well and, therefore, the calculated values will be used in the assessment of the exposure of the vessel itself.

Neutron exposure projections at key locations on the pressure vessel inner radius are given in Table 6-13. Along with the current (9.18 EFPY) exposure projections are also provided for an exposure period of 20 EFPY and to end of vessel design life (32 EFPY). The time averaged exposure rates for low leakage fuel cycles were used to perform projections beyond the end of the cycle 1 through 10 exposure period.

In the calculation of exposure gradients for use in the development of heatup and cooldown curves for the Zion Unit 2 reactor coolant system, exposure projections to 20 EFPY and 32 EFPY were employed. Data based on both a fluence (E > 1.0 MeV) slope and a plant specific dpa slope through the vessel wall are provided in Table 6-14. In order to access RT_{NDT} vs. fluence trend curves, dpa equivalent fast neutron fluence levels for the 1/4T and 3/4T positions were defined by the relations

$$\Phi' \text{ (1/4T)} = \Phi \text{ (Surface)} \left\{ \frac{\text{dpa (1/4T)}}{\text{dpa (Surface)}} \right\}$$

$$\Phi' \text{ (3/4T)} = \Phi \text{ (Surface)} \left\{ \frac{\text{dpa (3/4T)}}{\text{dpa (Surface)}} \right\}$$

Using this approach results in the dpa equivalent fluence values listed in Table 6-14.

In Table 6-15 updated lead factors are listed for each of the Zion Unit 2 surveillance capsules. These data may be used as a guide in establishing future withdrawal schedules for the remaining capsules.

NOTE: ALL DIMENSIONS ARE IN CENTIMETERS

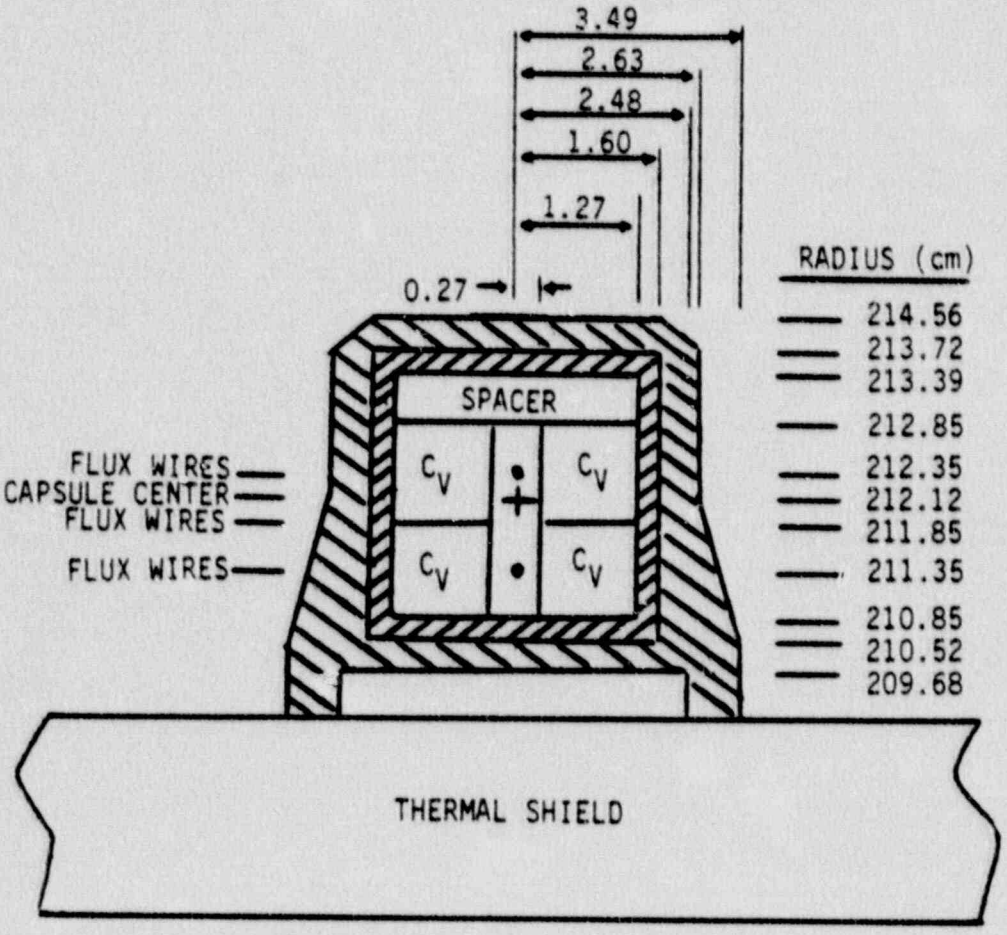

Figure 6-1 Plan View of a Reactor Vessel Surveillance Capsule

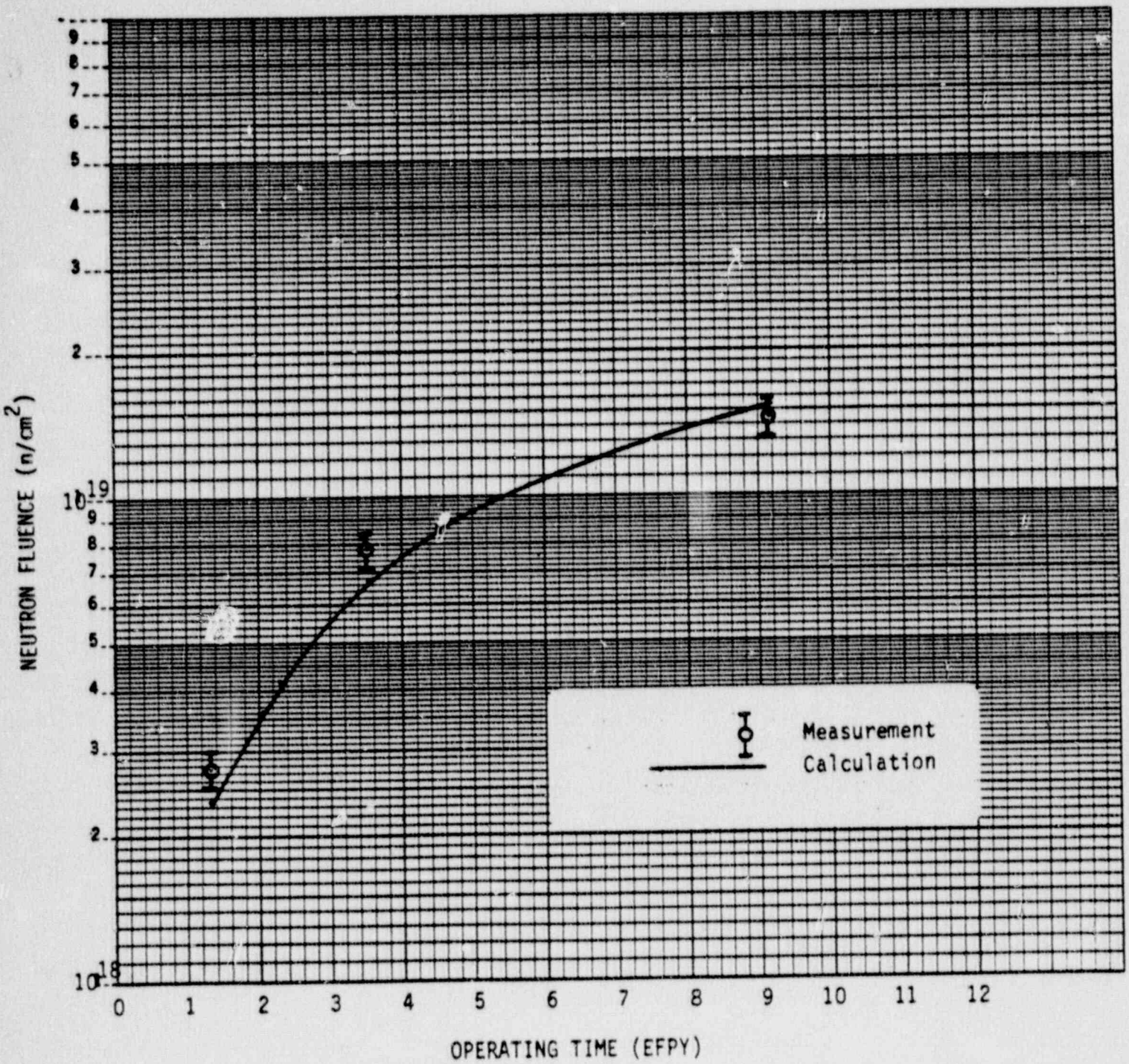

Figure 6-2. Fast Neutron (E >1.0 Mev) Fluence at the 40 Degree Surveillance Capsule Location as a Function of Full Power Operating Time

TABLE 6-1

CALCULATED FAST NEUTRON EXPOSURE PARAMETERS
AT THE SURVEILLANCE CAPSULE CENTER

	ϕ (E > 1.0 Mev)		ϕ(E > 0.1 Mev)		dpa/sec	
	Design Basis	Cycle 1-10	Design Basis	Cycle 1-10	Design Basis	Cycle 1-10
40° Capsule	7.54×10^{10}	5.45×10^{10}	2.22×10^{11}	1.63×10^{11}	1.24×10^{-10}	8.80×10^{-11}
4° Capsule	2.49×10^{10}	1.86×10^{10}	6.30×10^{10}	4.71×10^{10}	3.92×10^{-11}	2.92×10^{-11}

TABLE 6-2

CALCULATED FAST NEUTRON EXPOSURE PARAMETERS AT
THE PRESSURE VESSEL CLAD/BASE METAL INTERFACE

	ϕ (E > 1.0 Mev)		ϕ(E > 0.1 Mev)		dpa/sec	
	Design Basis	Cycle 1-10	Design Basis	Cycle 1-10	Design Basis	Cycle 1-10
45°	2.49×10^{10}	1.84×10^{10}	6.64×10^{10}	4.91×10^{10}	4.06×10^{-11}	3.00×10^{-11}
30°	1.61×10^{10}	1.20×10^{10}	4.13×10^{10}	3.08×10^{10}	2.60×10^{-11}	1.94×10^{-11}
15°	1.30×10^{10}	9.82×10^{9}	3.25×10^{10}	2.46×10^{10}	2.09×10^{-11}	1.58×10^{-11}
0°	8.02×10^{9}	5.98×10^{9}	2.02×10^{10}	1.51×10^{10}	1.31×10^{-11}	9.77×10^{-12}

TABLE 6-3

RELATIVE RADIAL DISTRIBUTIONS OF NEUTRON FLUX (E > 1.0 MeV)
WITHIN THE PRESSURE VESSEL WALL

Radius (cm)	0°	15°	30°	45°
220.27(1)	1.00	1.00	1.00	1.00
220.64	0.977	0.978	0.979	0.977
221.66	0.884	0.887	0.889	0.885
222.99	0.758	0.762	0.765	0.756
224.31	0.641	0.644	0.648	0.637
225.63	0.537	0.540	0.545	0.534
226.95	0.448	0.451	0.455	0.443
228.28	0.372	0.373	0.379	0.367
229.60	0.309	0.310	0.315	0.303
230.92	0.255	0.257	0.261	0.250
232.25	0.211	0.212	0.216	0.206
233.57	0.174	0.175	0.178	0.169
234.89	0.143	0.144	0.147	0.138
236.22	0.117	0.118	0.121	0.113
237.54	0.0961	0.0963	0.0989	0.0912
238.86	0.0783	0.0783	0.0807	0.0736
240.19	0.0635	0.0632	0.0656	0.0584
241.51	0.0511	0.0501	0.0519	0.0454
242.17(2)	0.0483	0.0469	0.0487	0.0422

NOTES: 1) Base Metal Inner Radius
2) Base Metal Outer Radius

TABLE 6-4

RELATIVE RADIAL DISTRIBUTIONS OF NEUTRON FLUX (E > 0.1 MeV)
WITHIN THE PRESSURE VESSEL WALL

Radius (cm)	0°	15°	30°	45°
220.27(1)	1.00	1.00	1.00	1.00
220.64	1.00	1.00	1.00	1.00
221.66	1.00	0.996	1.00	0.994
222.99	0.965	0.958	0.968	0.953
224.31	0.916	0.906	0.919	0.898
225.63	0.861	0.849	0.865	0.838
226.95	0.803	0.790	0.809	0.777
228.28	0.746	0.732	0.752	0.717
229.60	0.689	0.675	0.695	0.657
230.92	0.633	0.619	0.640	0.600
232.25	0.578	0.565	0.586	0.544
233.57	0.525	0.513	0.534	0.490
234.89	0.474	0.463	0.483	0.437
236.22	0.424	0.414	0.433	0.387
237.54	0.375	0.367	0.385	0.338
238.86	0.328	0.322	0.338	0.291
240.19	0.283	0.277	0.292	0.244
241.51	0.239	0.232	0.245	0.196
242.17(2)	0.229	0.220	0.232	0.183

NOTES: 1) Base Metal Inner Radius
2) Base Metal Outer Radius

TABLE 6-5

RELATIVE RADIAL DISTRIBUTIONS OF IRON DISPLACEMENT RATE (dpa) WITHIN THE PRESSURE VESSEL WALL

Radius (cm)	0°	15°	30°	45°
220.27(1)	1.00	1.00	1.00	1.00
220.64	0.983	0.983	0.984	0.983
221.66	0.913	0.914	0.918	0.915
222.99	0.818	0.819	0.827	0.820
224.31	0.728	0.728	0.739	0.730
225.63	0.647	0.646	0.659	0.647
226.95	0.574	0.573	0.587	0.573
228.28	0.510	0.507	0.523	0.507
229.60	0.453	0.450	0.466	0.449
230.92	0.402	0.399	0.414	0.397
232.25	0.356	0.353	0.368	0.349
233.57	0.315	0.312	0.327	0.307
234.89	0.277	0.275	0.289	0.269
236.22	0.243	0.241	0.254	0.233
237.54	0.212	0.210	0.222	0.201
238.86	0.182	0.181	0.192	0.170
240.19	0.155	0.154	0.164	0.141
241.51	0.131	0.128	0.137	0.113
242.17(2)	0.125	0.122	0.130	0.106

NOTES: 1) Base Metal Inner Radius
2) Base Metal Outer Radius

TABLE 6-6

NUCLEAR PARAMETERS FOR NEUTRON FLUX MONITORS

Monitor Material	Reaction of Interest	Target Weight Fraction	Response Range	Product Half-Life	Fission Yield (%)
Copper	$Cu^{63}(n,\alpha)Co^{60}$	0.6917	E> 4.7 MeV	5.272 yrs	
Iron	$Fe^{54}(n,p)Mn^{54}$	0.0582	E> 1.0 MeV	312.2 days	
Nickel	$Ni^{58}(n,p)Co^{58}$	0.6830	E> 1.0 MeV	70.90 days	
Uranium-238*	$U^{238}(n,f)Cs^{137}$	1.0	E> 0.4 MeV	30.12 yrs	5.99
Neptunium-237*	$Np^{237}(n,f)Cs^{137}$	1.0	E> 0.08 MeV	30.12 yrs	6.50
Cobalt-Aluminum*	$Co^{59}(n,\gamma)Co^{60}$	0.0015	0.4ev <E< 0.015 MeV	5.272 yrs	
Cobalt-Aluminum*	$Co^{59}(n,\gamma)Co^{60}$	0.0015	E < 0.015 MeV	5.272 yrs	

*Denotes that monitor is cadmium shielded.

TABLE 6-7

IRRADIATION HISTORY OF NEUTRON SENSORS
CONTAINED IN CAPSULE Y

Month	Year	PJ (MW)	PJ/PMAX	Irradiation Time (days)	Decay Time (days)
12	1973	305.5	0.0940	8	5616
1	1974	394.2	0.1213	31	5585
2	1974	436.4	0.1343	28	5557
3	1974	394.2	0.1213	31	5526
4	1974	219.0	0.0674	30	5496
5	1974	0.0	0.0000	31	5465
6	1974	0.0	0.0000	30	5435
7	1974	0.0	0.0000	31	5404
8	1974	76.9	0.0237	31	5373
9	1974	998.0	0.3071	30	5343
10	1974	849.6	0.2614	31	5312
11	1974	2243.2	0.6902	30	5282
12	1974	1073.5	0.3303	31	5251
1	1975	1637.2	0.5037	31	5220
2	1975	1765.6	0.5433	28	5192
3	1975	1776.8	0.5467	31	5161
4	1975	1550.6	0.4771	30	5131
5	1975	1950.6	0.6002	31	5100
6	1975	452.0	0.1391	30	5070
7	1975	2631.2	0.8096	31	5039
8	1975	2434.3	0.7490	31	5008
9	1975	635.6	0.1956	30	4978
10	1975	2366.4	0.7281	31	4947
11	1975	2499.3	0.7690	30	4917
12	1975	2321.1	0.7142	31	4886
1	1976	925.4	0.2847	31	4855
2	1976	1269.8	0.3907	29	4826
3	1976	2764.6	0.8506	31	4795
4	1976	31.4	0.0097	30	4765
5	1976	1754.8	0.5399	31	4734
6	1976	1612.0	0.4960	30	4704
7	1976	3093.1	0.9517	31	4673
8	1976	2351.3	0.7235	31	4642
9	1976	1510.4	0.4647	30	4612
10	1976	122.2	0.0376	31	4581
11	1976	3131.5	0.9635	30	4551
12	1976	2522.3	0.7761	31	4520

TABLE 6-7 - cont'd

IRRADIATION HISTORY OF NEUTRON SENSORS
CONTAINED IN CAPSULE Y

Month	Year	PJ (MW)	PJ/PMAX	Irradiation Time (days)	Decay Time (days)
1	1977	524.3	0.1613	31	4489
2	1977	0.0	0.0000	28	4461
3	1977	162.8	0.0501	31	4430
4	1977	2645.5	0.8140	30	4400
5	1977	3153.0	0.9702	31	4369
6	1977	2882.8	0.8870	30	4339
7	1977	2762.2	0.8499	31	4308
8	1977	3190.4	0.9817	31	4277
9	1977	3227.7	0.9932	30	4247
10	1977	3084.2	0.9490	31	4216
11	1977	3062.7	0.9424	30	4186
12	1977	2848.2	0.8764	31	4155
1	1978	2635.6	0.8110	31	4124
2	1978	220.9	0.0680	28	4096
3	1978	0.0	0.0000	31	4065
4	1978	1248.9	0.3843	30	4035
5	1978	3180.9	0.9787	31	4004
6	1978	3127.9	0.9624	30	3974
7	1978	3122.1	0.9606	31	3943
8	1978	3234.1	0.9951	31	3912
9	1978	3147.3	0.9684	30	3882
10	1978	3090.1	0.9508	31	3851
11	1978	3239.6	0.9968	30	3821
12	1978	3158.3	0.9718	31	3790
1	1979	2785.2	0.8570	31	3759
2	1979	1362.4	0.4192	28	3731
3	1979	312.8	0.0962	31	3700
4	1979	947.9	0.2917	30	3670
5	1979	2725.3	0.8385	31	3639
6	1979	2731.8	0.8406	30	3609
7	1979	2780.2	0.8554	31	3578
8	1979	2786.3	0.8573	31	3547
9	1979	2843.1	0.8748	30	3517
10	1979	1798.7	0.5534	31	3486
11	1979	0.0	0.0000	30	3456
12	1979	0.0	0.0000	31	3425

TABLE 6-7 - cont'd

IRRADIATION HISTORY OF NEUTRON SENSORS
CONTAINED IN CAPSULE Y

Month	Year	PJ (MW)	PJ/PMAX	Irradiation Time (days)	Decay Time (days)
1	1980	1069.0	0.3289	31	3394
2	1980	3131.4	0.9635	29	3365
3	1980	3175.6	0.9771	31	3334
4	1980	2745.4	0.8448	30	3304
5	1980	91.2	0.0281	31	3273
6	1980	0.0	0.0000	30	3243
7	1980	302.1	0.0929	31	3212
8	1980	2633.7	0.8104	31	3181
9	1980	2720.5	0.8371	30	3151
10	1980	2997.7	0.9224	31	3120
11	1980	2572.4	0.7915	30	3090
12	1980	2509.3	0.7721	31	3059
1	1981	2812.4	0.8653	31	3028
2	1981	2966.1	0.9126	28	3000
3	1981	2854.6	0.8783	31	2969
4	1981	2906.9	0.8944	30	2939
5	1981	2810.3	0.8647	31	2908
6	1981	2962.6	0.9116	30	2878
7	1981	2777.4	0.8546	31	2847
8	1981	2164.0	0.6658	31	2816
9	1981	566.5	0.1743	30	2786
10	1981	0.0	0.0000	31	2755
11	1981	6.3	0.0019	30	2725
12	1981	1485.9	0.4572	31	2694
1	1982	1533.6	0.4719	31	2663
2	1982	342.9	0.1055	28	2635
3	1982	543.7	0.1673	31	2604
4	1982	2120.3	0.6524	30	2574
5	1982	3098.8	0.9535	31	2543
6	1982	2071.6	0.6374	30	2513
7	1982	2730.2	0.8401	31	2482
8	1982	3122.9	0.9609	31	2451
9	1982	699.2	0.2151	30	2421
10	1982	795.4	0.2447	31	2390
11	1982	3229.7	0.9937	30	2360
12	1982	2945.8	0.9064	31	2329

TABLE 6-7 - cont'd

IRRADIATION HISTORY OF NEUTRON SENSORS
CONTAINED IN CAPSULE Y

Month	Year	PJ (MW)	PJ/PMAX	Irradiation Time (days)	Decay Time (days)
1	1983	3080.4	0.9478	31	2298
2	1983	2557.5	0.7869	28	2270
3	1983	0.0	0.0000	31	2239
4	1983	0.0	0.0000	30	2209
5	1983	207.5	0.0638	31	2178
6	1983	3001.5	0.9235	30	2148
7	1983	3066.5	0.9435	31	2117
8	1983	3021.4	0.9297	31	2086
9	1983	3222.9	0.9917	30	2056
10	1983	3227.7	0.9932	31	2025
11	1983	2835.5	0.8725	30	1995
12	1983	3226.5	0.9928	31	1964
1	1984	2928.0	0.9009	31	1933
2	1984	3226.5	0.9928	29	1904
3	1984	2393.6	0.7365	31	1873
4	1984	0.0	0.0000	30	1843
5	1984	0.0	0.0000	31	1812
6	1984	0.0	0.0000	30	1782
7	1984	1793.9	0.5520	31	1751
8	1984	3080.5	0.9479	31	1720
9	1984	3165.4	0.9740	30	1690
10	1984	3214.7	0.9891	31	1659
11	1984	3218.7	0.9904	30	1629
12	1984	3174.1	0.9766	31	1598
1	1985	3163.2	0.9733	31	1567
2	1985	3194.7	0.9830	28	1539
3	1985	3055.3	0.9401	31	1508
4	1985	3206.3	0.9866	30	1478
5	1985	3065.5	0.9432	31	1447
6	1985	2983.3	0.9179	30	1417
7	1985	2300.5	0.7078	31	1386
8	1985	1637.9	0.5040	31	1355
9	1985	182.4	0.0561	30	1325
10	1985	0.0	0.0000	31	1294
11	1985	0.0	0.0000	30	1264
12	1985	0.0	0.0000	31	1233

TABLE 6-7 - cont'd

IRRADIATION HISTORY OF NEUTRON SENSORS
CONTAINED IN CAPSULE Y

Month	Year	PJ (MW)	PJ/PMAX	Irradiation Time (days)	Decay Time (days)
1	1986	0.0	0.0000	31	1202
2	1986	2169.0	0.6674	28	1174
3	1986	2813.0	0.8655	31	1143
4	1986	3188.0	0.9809	30	1113
5	1986	3043.7	0.9365	31	1082
6	1986	2788.8	0.8581	30	1052
7	1986	1737.8	0.5347	31	1021
8	1986	3216.8	0.9898	31	990
9	1986	2838.3	0.8733	30	960
10	1986	3217.9	0.9901	31	929
11	1986	3227.3	0.9930	30	899
12	1986	3226.5	0.9928	31	868
1	1987	3226.7	0.9928	31	837
2	1987	2870.9	0.8833	28	809
3	1987	2007.2	0.6176	31	778
4	1987	0.0	0.0000	30	748
5	1987	0.0	0.0000	31	717
6	1987	0.0	0.0000	30	687
7	1987	0.0	0.0000	31	656
8	1987	1937.8	0.59[illegible]	31	625
9	1987	3168.4	0.9[illegible]	30	595
10	1987	2653.4	0.8164	31	564
11	1987	3151.4	0.9697	30	534
12	1987	3049.2	0.9382	31	503
1	1988	3142.8	0.9670	31	472
2	1988	3121.3	0.9604	29	443
3	1988	2920.1	0.8985	31	412
4	1988	2906.9	0.8944	30	382
5	1988	3082.5	0.9484	31	351
6	1988	3176.0	0.9772	30	321
7	1988	3214.1	0.9889	31	290
8	1988	2694.2	0.8290	31	259
9	1988	3166.3	0.9742	30	229
10	1988	1950.3	0.6001	13	216

TABLE 6-8

MEASURED SENSOR ACTIVITIES AND REACTION RATES

Monitor and Axial Location	Measured Activity (dis/sec-gm)	Adjusted Saturated Activity (dis/sec-gm)	Reaction Rate (RPS/NUCLEUS)
Cu-63 (n,α) Co-60			
Middle	1.32×10^{5}	2.78×10^{5}	
Bottom-Middle	1.36×10^{5}	2.86×10^{5}	
Average	1.34×10^{5}	2.82×10^{5}	4.30×10^{-17}
Fe-54(n,p) Mn-54			
Top	1.10×10^{6}	2.52×10^{6}	
Top-Middle	1.12×10^{6}	2.56×106	
Middle	1.08×10^{6}	2.47×10^{6}	
Bottom-Middle	1.14×10^{6}	2.61×10^{6}	
Bottom	1.10×10^{6}	2.52×10^{6}	
Average	1.11×10^{6}	2.54×10^{6}	4.04×10^{-15}
Ni-58 (n,p) Co-58			
Top-Middle	4.22×10^{6}	3.94×10^{7}	
Middle	4.21×10^{6}	3.93×10^{7}	
Bottom-Middle	4.31×10^{6}	4.02×10^{7}	
Average	4.25×10^{6}	3.96×10^{7}	5.65×10^{-15}
U-238 (n,f) Cs-137 (Cd)			
Middle	4.09×10^{5}	2.31×10^{6}	1.52×10^{-14}

TABLE 6-8

MEASURED SENSOR ACTIVITIES AND REACTION RATES - cont'd

Monitor and Axial Location	Measured Activity (dis/sec-gm)	Saturated Activity (dis/sec-gm)	Reaction Rate (RPS/NUCLEUS)
Np-237(n,f) Cs-137 (Cd)			
Middle	3.88×10^{6}	2.19×10^{7}	1.33×10^{-13}
Co-59 (n,γ) Co-60 (Cd)			
Top	1.23×10^{7}	2.47×10^{7}	
Average	1.23×10^{7}	2.47×10^{7}	1.61×10^{-12}

TABLE 6-9

SUMMARY OF NEUTRON DOSIMETRY RESULTS

	TIME AVERAGED EXPOSURE RATES	
ϕ (E> 1.0 MeV) {n/cm^2-sec}	5.10×10^{10}	± 8%
ϕ (E> 0.1 MeV) {n/cm^2-sec}	1.64×10^{11}	± 15%
dpa/sec	8.47×10^{-11}	± 10%
	INTEGRATED CAPSULE EXPOSURE	
ϕ (E> 1.0 MeV) {n/cm^2}	1.48×10^{19}	± 8%
ϕ (E> 0.1 MeV) {n/cm^2}	4.76×10^{19}	± 15%
dpa	2.45×10^{-2}	± 10%

NOTE: Total Irradiation Time = 9.18 EFPY

TABLE 6-10

COMPARISON OF MEASURED AND FERRET CALCULATED
REACTION RATES AT THE SURVEILLANCE CAPSULE CENTER

Reaction	Measured	Adjusted Calculation	C/M
Cu-63 (n,α) Co-60	4.30×10^{-17}	4.34×10^{-17}	1.01
Fe-54 (n,p) Mn-54	4.04×10^{-15}	3.98×10^{-15}	0.98
Ni-58 (n,p) Co-58	5.65×10^{-15}	5.49×10^{-15}	0.97
U-238 (n,f) Cs-137 (Cd)	1.52×10^{-14}	1.77×10^{-14}	1.16
Np-237 (n,f) Cs-137 (Cd)	1.33×10^{-13}	1.36×10^{-13}	1.02
Co-59 (n,γ) Co-60 (Cd)	1.61×10^{-12}	1.59×10^{-12}	0.99

TABLE 6-11

ADJUSTED NEUTRON ENERGY SPECTRUM AT THE SURVEILLANCE CAPSULE CENTER

Group	Energy (Mev)	Adjusted Flux (n/cm^2-sec)	Group	Energy (Mev)	Adjusted Flux (n/cm^2-sec)
1	1.73×10^{1}	6.45×10^{6}	28	9.12×10^{-3}	7.63×10^{9}
2	1.49×10^{1}	1.49×10^{7}	29	5.53×10^{-3}	9.16×10^{9}
3	1.35×10^{1}	5.49×10^{7}	30	3.36×10^{-3}	2.89×10^{9}
4	1.16×10^{1}	1.23×10^{8}	31	2.84×10^{-3}	2.79×10^{9}
5	1.00×10^{1}	2.71×10^{8}	32	2.40×10^{-3}	2.75×10^{9}
6	8.61×10^{0}	4.63×10^{8}	33	2.04×10^{-3}	8.24×10^{9}
7	7.41×10^{0}	1.07×10^{9}	34	1.23×10^{-3}	8.45×10^{9}
8	6.07×10^{0}	1.54×10^{9}	35	7.49×10^{-4}	8.71×10^{9}
9	4.97×10^{0}	3.10×10^{9}	36	4.54×10^{-4}	8.98×10^{9}
10	3.68×10^{0}	3.68×10^{9}	37	2.75×10^{-4}	9.70×10^{9}
11	2.87×10^{0}	6.92×10^{9}	38	1.67×10^{-4}	1.23×10^{10}
12	2.23×10^{0}	7.98×10^{9}	39	1.01×10^{-4}	1.03×10^{10}
13	1.74×10^{0}	9.78×10^{9}	40	6.14×10^{-5}	9.97×10^{9}
14	1.35×10^{0}	9.21×10^{9}	41	3.73×10^{-5}	9.50×10^{9}
15	1.11×10^{0}	1.49×10^{10}	42	2.26×10^{-5}	8.99×10^{9}
16	8.21×10^{-1}	1.52×10^{10}	43	1.37×10^{-5}	8.54×10^{9}
17	6.39×10^{-1}	1.47×10^{10}	44	8.32×10^{-6}	8.11×10^{9}
18	4.98×10^{-1}	1.04×10^{10}	45	5.04×10^{-6}	7.67×10^{9}
19	3.88×10^{-1}	1.27×10^{10}	46	3.06×10^{-6}	7.29×10^{9}
20	3.02×10^{-1}	1.66×10^{10}	47	1.86×10^{-6}	6.85×10^{9}
21	1.83×10^{-1}	1.51×10^{10}	48	1.13×10^{-6}	5.91×10^{9}
22	1.11×10^{-1}	1.23×10^{10}	49	6.83×10^{-7}	5.73×10^{9}
23	6.74×10^{-2}	9.58×10^{9}	50	4.14×10^{-7}	8.60×10^{9}
24	4.09×10^{-2}	6.48×10^{9}	51	2.51×10^{-7}	9.47×10^{9}
25	2.55×10^{-2}	6.21×10^{9}	52	1.52×10^{-7}	1.05×10^{10}
26	1.99×10^{-2}	4.22×10^{9}	53	9.24×10^{-8}	3.20×10^{10}
27	1.50×10^{-2}	6.32×10^{9}			

NOTE: Tabulated energy levels represent the upper energy of each group.

TABLE 6-12

COMPARISON OF CALCULATED AND MEASURED
EXPOSURE LEVELS FOR SURVEILLANCE CAPSULE

	CAPSULE Y		
	Calculated	Measured	C/M
Φ(E> 1.0 MeV) {n/cm^2}	1.58×10^{19}	1.48×10^{19}	1.07
Φ(E> 0.1 MeV) {n/cm^2}	4.71×10^{19}	4.76×10^{19}	0.99
dpa	2.55×10^{-2}	2.46×10^{-2}	1.04

	CAPSULE T		
	Calculated	Measured	C/M
Φ(E> 1.0 MeV) {n/cm^2}	6.70×10^{18}	7.81×10^{18}	0.86
Φ(E> 0.1 MeV) {n/cm^2}	2.00×10^{19}	2.51×10^{19}	0.80
dpa	1.08×10^{-2}	1.29×10^{-2}	0.84

	CAPSULE U		
	Calculated	Measured	C/M
Φ(E> 1.0 MeV) {n/cm^2}	2.34×10^{18}	2.73×10^{18}	0.86
Φ(E> 0.1 MeV) {n/cm^2}	6.98×10^{18}	8.56×10^{18}	0.82
dpa	3.78×10^{-2}	4.43×10^{-3}	0.85

TABLE 6-13
NEUTRON EXPOSURE PROJECTIONS AT KEY LOCATIONS
ON THE PRESSURE VESSEL CLAD/BASE METAL INTERFACE

	AZIMUTHAL ANGLE			
	0°	15°	30°	45°
9.18 EFPY				
Φ(E> 1.0 MeV) (n/cm^2)	1.73×10^{18}	2.85×10^{18}	3.48×10^{18}	5.34×10^{18}
Φ(E> 0.1 MeV) (n/cm^2)	4.38×10^{18}	7.13×10^{18}	8.93×10^{18}	1.42×10^{19}
dpa	2.83×10^{-3}	4.58×10^{-3}	5.63×10^{-3}	8.70×10^{-3}
20.0 EFPY				
Φ(E> 1.0 MeV) (n/cm^2)	3.47×10^{18}	5.85×10^{18}	7.20×10^{18}	1.11×10^{19}
Φ(E> 0.1 MeV) (n/cm^2)	8.77×10^{18}	1.47×10^{19}	1.85×10^{19}	2.97×10^{19}
dpa	5.57×10^{-3}	9.41×10^{-3}	1.16×10^{-2}	1.81×10^{-2}
32.0 EFPY				
Φ(E> 1.0 MeV) (n/cm^2)	5.41×10^{18}	9.18×10^{18}	1.13×10^{19}	1.74×10^{19}
Φ(E> 0.1 MeV) (n/cm^2)	1.36×10^{19}	2.30×10^{19}	2.91×10^{19}	4.65×10^{19}
dpa	8.83×10^{-3}	1.47×10^{-2}	1.83×10^{-2}	2.84×10^{-2}

TABLE 6-14

NEUTRON EXPOSURE VALUES FOR USE IN THE GENERATION OF HEATUP/COOLDOWN CURVES

20 EFPY

	NEUTRON FLUENCE (E > 1.0 MeV) SLOPE (n/cm^2)			dpa SLOPE (equivalent n/cm^2)		
	Surface	1/4 T	3/4 T	Surface	1/4 T	3/4 T
0°	3.47×10^{18}	1.83×10^{18}	3.78×10^{17}	3.47×10^{18}	2.22×10^{18}	8.05×10^{17}
15°	5.85×10^{18}	3.11×10^{18}	6.44×10^{17}	5.85×10^{18}	3.74×10^{18}	1.34×10^{18}
30°	7.20×10^{18}	3.87×10^{18}	8.13×10^{17}	7.20×01^{18}	4.70×10^{18}	1.74×10^{18}
45°	1.11×10^{19}	5.84×10^{18}	1.16×10^{18}	1.11×10^{19}	7.10×10^{18}	2.45×10^{18}

32 EFPY

	NEUTRON FLUENCE (E > 1.0 MeV) SLOPE (n/cm^2)			dpa SLOPE (equivalent n/cm^2)		
	Surface	1/4 T	3/4 T	Surface	1/4 T	3/4 T
0°	5.41×10^{18}	2.86×10^{18}	5.89×10^{17}	5.41×10^{18}	3.46×10^{18}	1.26×10^{18}
15°	9.18×10^{18}	4.88×10^{18}	1.01×10^{18}	9.18×10^{18}	5.87×10^{18}	2.11×10^{18}
30°	1.13×10^{19}	6.07×10^{18}	1.27×10^{18}	1.13×01^{19}	7.37×10^{18}	2.73×10^{18}
45°	1.74×10^{19}	9.15×10^{18}	1.82×10^{18}	1.74×10^{19}	1.11×10^{19}	3.84×10^{18}

TABLE 6-15

UPDATED LEAD FACTORS FOR ZION
UNIT 2 SURVEILLANCE CAPSULES

Capsule	Lead Factor
U	Withdrawn
T	Withdrawn
Y	Withdrawn
X	2.97
W	1.01
V	1.01
Z	1.01
S	1.01

SECTION 7.0
SURVEILLANCE CAPSULE REMOVAL SCHEDULE

The following removal schedule meets ASTM E185-82 and is recommended for future capsules to be removed from the Zion Unit 2 reactor vessel:

Capsule	Location (deg.)	Capsule Lead Factor	Removal Time (a)	Estimated Fluence (n/cm^2)
U	140	2.97	1.27 (Removed)	2.73×10^{18}
T	40	2.97	3.56 (Removed)	7.81×10^{18} (b)
Y	320	2.97	9.18 (Removed	1.48×10^{19} (c)
X	220	2.97	15	2.42×10^{19}
W	184	1.01	Standby	-
V	176	1.01	Standby	-
Z	356	1.01	Standby	-
S	4	1.01	Standby	-

(a) Effective full power years from plant startup.

(b) Approximate fluence at 1/4 thickness reactor vessel wall at end of life.

(c) Approximate fluence at reactor vessel inner wall at end of life.

8.0 REFERENCES

1. S. E. Yanichko and D. L. Lege, "Commonwealth Edison Co. Zion Unit No. 2 Reactor Vessel Radiation Surveillance Program", WCAP-8132, May 1973.

2. Perrin, Farmelo, Jung and Fromm, "Zion Nuclear Plant Reactor Pressure Vessel Surveillance Program: Unit No. 1 Capsule T, and Unit No. 2 Capsule U", BCL-585-4, March 1978.

3. E. B. Norris, "Reactor Vessel Material Surveillance Program For Zion Unit No. 2 Analysis of Capsule T", SwRI Project No. 06-6901-001, July 1983.

4. Code of Federal Regulations, 10CFR50, Appendix G, "Fracture Toughness Requirements," and Appendix H, "Reactor Vessel Material Surveillance Program Requirements," U.S. Nuclear Regulatory Commission, Washington, D.C.

5. Regulatory Guide 1.99, Proposed Revision 2, "Radiation Damage to Reactor Vessel Materials," U.S. Nuclear Regulatory Commission, February 1986.

6. R. G. Soltesz, R. K. Disney, J. Jedruch, and S. L. Ziegler, "Nuclear Rocket Shielding Methods, Modification, Updating and Input Data Preparation. Vol. 5--Two-Dimensional Discrete Ordinates Transport Technique", WANL-PR(LL)-034, Vol. 5, August 1970.

7. "ORNL RSCI Data Library Collection DLC-76, SAILOR Coupled Self-Shielded, 47 Neutron, 20 Gamma-Ray, P3, Cross Section Library for Light Water Reactors".

8. S. Altomore, et al., "Core Physics Characteristics of the Zion Station Nuclear Plants (Units 1 and 2, Cycle 1), WCAP-7675, November 1971. (Proprietary)

9. T. L. Wheeler, et al., "Core Physics Characteristics of the Zion Station Nuclear Plant (Unit 2, Cycle 2)," WCAP-8881, November 1976. (Proprietary)

10. T. L. Wheeler, et al., "Core Physics Characteristics of the Zion Station Nuclear Plant Unit 2 (COM), Cycle 3," WCAP-9246, December 1977. (Proprietary)

11. W. F. Staley, et al., "Core Physics Characteristics of the Zion Station Nuclear Plant Unit 2 (COM), Cycle 4," WCAP-9458, January 1979. (Proprietary)

12. C. A. Grier, et al., "Core Physics Characteristics of the Zion Station Nuclear Plant Unit 2 (COM), Cycle 5," WCAP-9687, April 1980. (Proprietary)

13. D. L. Maret, et al., "Core Physics Characteristics of the Zion Station Nuclear Plant (Unit 2, Cycle 6)," WCAP-9959, August 1981. (Proprietary)

14. D. J. Wanner, et al., "Core Physics Characteristics of the Zion Station Nuclear Plant (Unit 2, Cycle 7)," WCAP-10282, February 1983. (Proprietary)

15. D. K. Lee, et. al., "Nuclear Design Report for Zion Unit 2, Cycle 8," NFSR-0024, May 1984. (CECo. Proprietary)

16. D. K. Lee, et al., "Nuclear Design Report for Zion Unit 2, Cycle 9," NFSR-0037, December 1985. (CECo. Proprietary)

17. D. K. Lee, et al., "Nuclear Design Report for Zion Unit 2, Cycle 10," NFSR-0052, December 1985. (CECo. Proprietary)

18. ASTM Designation E482-82, "Standard Guide for Application of Neutron Transport Methods for Reactor Vessel Surveillance", in ASTM Standards, Section 12, American Society for Testing and Materials, Philadelphia, PA, 1984.

19. ASTM Designation E560-77, "Standard Recommended Practice for Extrapolating Reactor Vessel Surveillance Dosimetry Results", in ASTM Standards, Section 12, American Society for Testing and Materials, Philadelphia, PA, 1984.

20. ASTM Designation E693-79, "Standard Practice for Characterizing Neutron Exposures in Ferritic Steels in Terms of Displacements per Atom (dpa)", in ASTM Standards, Section 12, American Society for Testing and Materials, Philadelphia, PA, 1984.

21. ASTM Designation E706-81a, "Standard Master Matrix for Light-Water Reactor Pressure Vessel Surveillance Standard", in ASTM Standards, Section 12, American Society for Testing and Materials, Philadelphia, PA, 1984.

22. ASTM Designation E853-84, "Standard Practice for Analysis and Interpretation of Light-Water Reactor Surveillance Results", in ASTM Standards, Section 12, American Society for Testing and Materials, Philadelphia, PA, 1984.

23. ASTM Designation E261-77, "Standard Method for Determining Neutron Flux, Fluence, and Spectra by Radioactivation Techniques", in ASTM Standards, Section 12, American Society for Testing and Materials, Philadelphia, PA, 1984.

24. ASTM Designation E262-77, "Standard Method for Measuring Thermal Neutron Flux by Radioactivation Techniques", in ASTM Standards, Section 12, American Society for Testing and Materials, Philadelphia, PA, 1984.

25. ASTM Designation E263-82, "Standard Method for Determining Fast-Neutron Flux Density by Radioactivation of Iron", in ASTM Standards, Section 12, American Society for Testing and Materials, Philadelphia, PA, 1984.

26. ASTM Designation E264-82, "Standard Method for Determining Fast-Neutron Flux Density by Radioactivation of Nickel", in ASTM Standards, Section 12, American Society for Testing and Materials, Philadelphia, PA, 1984.

27. ASTM Designation E481-78, "Standard Method for Measuring Neutron-Flux Density by Radioactivation of Cobalt and Silver", in ASTM Standards, Section 12, American Society for Testing and Materials, Philadelphia, PA, 1984.

28. ASTM Designation E523-82, "Standard Method for Determining Fast-Neutron Flux Density by Radioactivation of Copper", in ASTM Standards, Section 12, American Society for Testing and Materials, Philadelphia, PA, 1984.

29. ASTM Designation E704-84, "Standard Method for Measuring Reaction Rates by Radioactivation of Uranium-238", in ASTM Standards, Section 12, American Society for Testing and Materials, Philadelphia, PA, 1984.

30. ASTM Designation E705-79, "Standard Method for Measuring Fast-Neutron Flux Density by Radioactivation of Neptunium-237", in ASTM Standards, Section 12, American Society for Testing and Materials, Philadelphia, PA, 1984.

31. ASTM Designation E1005-84, "Standard Method for Application and Analysis of Radiometric Monitors for Reactor Vessel Surveillance", in ASTM Standards, Section 12, American Society for Testing and Materials, Philadelphia, PA, 1984.

32. F. A. Schmittroth, FERRET Data Analysis Core, HEDL-TME 79-40, Hanford Engineering Development Laboratory, Richland, WA, September 1979.

33. W. N. McElroy, S. Berg and T. Crocket, A Computer-Automated Iterative Method of Neutron Flux Spectra Determined by Foil Activation, AFWL-TR-67-41, Vol. I-IV, Air Force Weapons Laboratory, Kirkland AFB, NM, July 1967.

34. EPRI-NP-2188, "Development and Demonstration of an Advanced Methodology for LWR Dosimetry Applications", R. E. Maerker, et al., 1981.